USING RECYCLED CONCRETE AGGREGATE IN PERVIOUS CONCRETE

By

KRISTYNA TYLOVA LANNON

A THESIS PRESENTED TO THE GRADUATE SCHOOL
OF THE UNIVERSITY OF FLORIDA IN PARTIAL FULFILLMENT
OF THE REQUIREMENTS FOR THE DEGREE OF
MASTER OF SCIENCE IN BUILDING CONSTRUCTION
UNIVERSITY OF FLORIDA

2009

To my husband, who has stood by me during my graduate study; my parents in Czech, my dear sister and my wonderful father-in-law

ACKNOWLEDGMENTS

First, I would like to thank Dr. Musinzky and Dr. Issa for guiding me through this thesis. I also have to express my appreciation for the help and facility resources landed to me by the material's research lab at the FDOT, namely by Mr. Craig Roberts. Thank you! An essential part of this thesis was the construction of the falling head permeameter, which would not have been possible without the kind donation of WW Gay, mechanical contractors.

I am most grateful to my dear friend Sarah Farmerie and her father, Dr. William Farmerie for their help, support and friendship.

Additionally, I thank the owners of Karma Cream for providing me with a safe and comfortable place to write this thesis.

TABLE OF CONTENTS

LIST OF TABLES

LIST OF FIGURES

LIST OF OBJECTS

LIST OF ABBREVIATIONS

GBFS	Granulated Blast Furnace Slag
FA	Fly Ash
W/C	Water to Cement Ratio
A/C	Aggregate to Cement Ratio
PC	Portland Cement
FDOT	Florida Department of Tramsportation
UK	United Kingdom
EPA	Environmental Protection Agency
RCA	Recycled Concrete Aggregate

Abstract of Thesis Presented to the Graduate School
of the University of Florida in Partial Fulfillment of the
Requirements for the Degree of Master of Science in Building Construction

USING RECYCLED CONCRETE AGGREGATE IN PERVIOUS CONCRETE

By

Kristyna Tylova Lannon

August 2009

Chair: Larry Muszynski
Cochair: Raymond R. Issa
Major: Building Construction

The subject of this thesis was to examine the possibility of further increasing the environmental benefits of an already existing environmentally friendly paving material, pervious concrete. This was attempted by replacing virgin aggregate with recycled concrete aggregate and also replacing portions of the Portland cement with industrial waste mineral admixtures, fly ash class F and granulated blast furnace slag.

Twelve pervious concrete mixes were designed with varying recycled concrete aggregate sizes and cementitious material blends. Three cylinders were poured per mix, each compacted by either rodding, vibration, or customized standard proctor method. Total of 36 samples were poured, cured, and tested. Tests were performed for Specific Gravity, Porosity (%), Permeability (in/s), and Compressive Strength (psi).

The 36 samples tested in this thesis were characterized by the following properties: 23.3 to 35.1% porosity, 0.5 to 1.9 in/s permeability, and 627 psi to 1325 psi compressive strength. Such results are consistent with properties collected from studies conducted on pervious concrete made with conventional aggregate. Therefore, demonstrating that recycled concrete aggregate and mineral admixtures can be successfully used in the production of pervious concrete.

CHAPTER 1
INTRODUCTION

Background

Two of the most important environmental issues of the present day are preserving / protecting clean water, and reducing / eliminating waste. Decreasing the amount of impervious surfaces in urban areas along with using recycled materials contributes to solving both problems.

The materials studied here are pervious concrete and recycled concrete aggregate. The most significant benefits of pervious concrete pavement are its ability to filtrate the "first flush" portion of stormwater, temporarily retain stormwater, in-filter and recharge ground waters. Using recycled concrete aggregate instead of virgin aggregate in pervious concrete diverts waste material from landfills and reduces the need for mining raw materials.

Research Hypothesis

If recycled concrete aggregate were used in the production of pervious concrete pavement, the environmental benefits of such pervious pavement would be increased by its recycled content. To farther reduce the environmental burden of concrete, caused by the high levels of CO_2 emissions released during the manufacturing processes of PC, industrial-waste mineral admixtures such as fly ash and blast furnace slag can be used to, in part, replace PC.

Research Objectives

This research will strive to answer the following questions:

- Will using recycled concrete aggregate instead of virgin aggregate compromise the integrity or the performance of previous concrete?
- Can a significant percentage of the Portland cement be replaced with industrial waste minerals, such as fly ash and blast furnace slag?
- How will the pervious concrete properties differ in respect to the aggregate size?
- How will the pervious concrete properties differ in respect to the compaction method?

CHAPTER 2
LITERATURE REVIEW

Introduction

The literature review for this research was conducted in two parts. First, studies regarding the history, applications, benefits, mixing practices and fresh and hardened properties of pervious concrete were reviewed and summarized. Second, the specifications, known properties and uses of recycled concrete aggregate were summed up.

Pervious concrete

General

Pervious concrete is described by the ACI as "zero-slump, open-graded material consisting of Portland cement, coarse aggregate, little or no fines aggregate, admixtures, and water" (ACI 2006). Other common names for pervious concrete are porous concrete or no-fines concrete. Pervious concrete has been introduced in the United States fairly recently and became popular as a paving system due to the "green" movement. It is most often used to resolve stormwater runoff issues and to reduce heat island effect.

History

The 1974 study conducted by V.M. Malhotra goes into a great detail concerning the history of pervious concrete. The oldest recorded pervious concrete structures are two houses built in the UK in 1852, using on-site found gravel, cement, and water. In the 1923, several multi-story dwellings constructed with pervious concrete surfaced again in UK. By the 1930s, pervious concrete structures could be found not only in UK but around most of Europe. However, it was the end of the Work War II (1945) and the subsequent shortage of building material that resulted in the first widespread interest in pervious concrete. (Malhotra 1976).

During its early days, pervious concrete was used mainly for load bearing, cast-in-place, exterior and retaining walls, and as sub-base for conventional concrete slabs. Due to such use, permeability is listed among the disadvantages along with low compressive and flexural strength. On the other hand, the list of benefits is still current today and includes: economy of material compared to conventional concrete (no fines, less cement, less water), lower shrinkage, lower unit weight and higher thermal insulating values due to the increased void content. (Malhotra 1976).

Design mix and porosity

In the past 30 years, many experiments have been cried out looking at different pervious concrete mixes and their properties. In general, all researchers agree that the most optimum design for pervious concrete used for pavement is made with 3/4" to 3/8" aggregate,15 to 35% of voids, and pores of 0.08 to 0.32 in. (ACI 2006, Ghafoori and Dutta 1995a, Chouch et al. 2007, Meininger 2004, Obla 2007). Table 2-1 summarizes the A/C and W/C ratios recommended by several researches. The A/C ratios are listed in terms of weight (w) or volume (v).

Table 2-1. A/C and W/C ratios recommended in the reviewed literature

Source	Aggregate size	A/C	W/C
Ghafoorie and Dutta 1995a	3/4" to 3/8"	4:1 (w) 4.5:1 (w) 5:1 (w) 6:1 (w)	0.37 0.38 0.39 0.42
Crouch et al. 2007	3/4" to 3/8"	4.47:1 to 5.64 (w)	0.30
Montes and Haselbach 2006	3/8" to 5/8"	4:1 (w)	0.25 to 0.26
Chopra et al. 2007	3/8" lime stone	4:1 to 7:1 (v)	0.33 to0.52
Meininger 1988			0.35 to 0.45

Since, pervious concrete has a lower amount of water then conventional concert, a care has to be taken when deciding the W/C ratio. Too little water will result in a week compressive strength mix with not enough paste to coat all aggregate. With too much water, the cement paste will be wattered down and settle, creating uneven strength thought the specimen, clogging the

bottom portion voids, and possibly creating impervious concrete.(ACI 2006, Ghafoori and Dutta 1995a). In addition, Meininger observed in his 1988 study that in mixes with inadequate water the cement paste sticks to the mixer more then in fully saturate cement paste mixes. The proper amount of water in the mix can be detected by "shiny metallic gleam" (Malhotra 1976).

Compressive Strength and Porosity

It is agreed that achieving balance between porosity (voids) and compressive strength is the single biggest challenge with mixing pervious concrete. Inconveniently, the compressive strength decreases as the porosity increases. Same as the compressive strength, the unit weight increases with compaction efforts while porosity and permeability decreases. (Chopra et al. 2007)

The study results found in the literature start to vary significantly when it comes to compressive strength. The compressive strengths reported range from 400 to 4000 psi, depending on the aggregate size and type, A/C and W/C ratios, and compaction efforts (ACI 2006, Chopra et al. 2007). The compaction method and energy has a considerable effect on the compressive strength. During compaction, a titer bond is formed among the aggregate creating a higher compressive strength. However, at the same time as aggregate is pressed closer together the size and amount of pores is reducec, thus decreasing the porosity.

Common compaction methods of pervious concrete are rodding (Malhotra 1976), compaction by a 5lb hammer (Ghaffoori and Dutta 1995a), 5.5lb standard proctor hammer, or by the 10 lb modified proctor hammer (Chapra et al. 2007). Table 2-2 lists the compaction methods, voids ratio, and compressive strength found in the literature.

Table 2-2. Compaction methods, compressive strength and void content found in literature

Source	Aggregate	Compaction method	Voids	Compressive Strength
Meininger 1988	no. 6 to no. 67	5 taps/2 layers/5lb hammer	-	980 to 1360
		15 taps/2 layers/5lb hammer	-	1400 to 1550
		Rodding	-	2100 to 2480
Crouch et al. 2007		3/8" to 3/4"	13% to 40%	870 to 5000

Meininger's study concludes that pervious concrete with 10 – 15% porosity will exhibit in little to no permeability but fairly high compressive strength (up to 4000psi). Pervious concrete with 15 – 20% porosity will result in optimum permeability and good strength (up to 2500), and 20 to 30% in more then adequate permeability, but very low compressive strength. Study performed by Obla in 2007, confirms that pervious concrete can achieve up to 4000 psi, but the usual strength achieved is around 2500 psi.

According to Crouch et al. (2007), samples made with narrow aggregate size distribution compact better and the smaller the aggregate the higher the compressive strength. Similar to conventional concrete, the compressive strength increases rapidly up to the 28^{th} day of curing and then levels off.

A study by Wang at al. 2006, concentrates on increasing the compressive strength of pervious concrete without compromising permeability. Some positive results were achieved by adding small amounts of fines, fibers and latex. The most success was realized in samples with 7% of fine sand, which increased the compressive strength on average by 46% while still maintaining adequate permeability. The finesse modulus of the river sand fines used was 2.9, the specific gravity was 2.62, and the absorption was 1.1%.

Permeability of Pervious Concrete System

The permeability, also called a drainage rate, can range from 2 to 18 gal/min/ft^2 (ACI 2006). Another common unit used for permeability is in/min., which is more relative to soil drainage and rainfall data. The hydraulic design for pervious pavement is almost always driven by the permeability of the soil not the concrete, as the permeability of most pervious concretes is much higher then that of even a saturated sand. For proper performance, the drainage rate of soil below pervious pavement should be no less then 0.5 in/hr. (EPA)

Uses

The most common use for pervious concrete today is in low traffic pavement such as parking lots, driveways, country roads, and sidewalks. Non the less, it is also used for greenhouse floors, tennis courts, zoo areas, animal barns and stalls, swimming pool decks, bridge embankments, beach structures and seawalls, sewage treatment plant sludge beds, solar energy storage systems and artificial reefs (ACI 2006). In addition, pervious concrete has also been used for military airport runways (Meithalath at al. 2003)

Pervious concrete pavements have been successfully used in Florida in low traffic pavements for the past two decades to reduce polluted stormwater runoff following heavy rain events. The pavement thickness for parking lots is recommended to be 5 to 10 inches, and 6 to 10 inches for plain roads. (ACI 2006)

Benefits

The major benefit of pervious concrete pavement is its ability to filter stormwater and reduce runoff. Even with pavements placed over less permeable soil, the first 30 minutes of a rain event (called the first flush), which produce the most polluted stormwater runoff, can be caught and temporarily stored in the pores of pervious concrete pavement (Obla 2007). This characteristic makes it possible for such pavement to replace basins and bio-swales, allowing for

more efficient land use. The porous nature of pervious concrete pavement is ideal for placement around trees and other plants, as it lets water and air through to reach the roots (Meininger 1988). The study done by Meithalath at al. in 2003 shows that pervious pavements can eliminate tire-road interaction noise as well as hydroplaning and glare. Additionally, pervious concrete pavements are significantly cooler then asphalt pavements (Diniz 1980), due to their lighter color and many voids. This is beneficial within urban areas where the temperature increases caused by impervious dark pavement become hazards.

Recent Developments

The first one of several proposed ASTM Standards for pervious concrete was released October 2008. It is the ASTM C1688 / C1688M - 08 Standard Test Method for Density and Void Content of Freshly Mixed Pervious Concrete. The new standard was developed to allow on-site check of the fresh pervious concrete mix before placement. According to Michael Davy, chair of the C09.49 task group who is in charge of developing the new series of pervious concrete standards: ” the new standard can be used as a means of verifying that the pervious concrete delivered to a project corresponds to the producer’s mix proportions.”

ASTM Standards guiding the testing of compressive strength, flexural strength, surface durability, hardened density, hardened void content, and field infiltration rate are still in the development phase (Palmer 2009). Francis T. Mayo, Director of Municipal Environmental Research Laboratory said: “ The development of porous pavement is a recognition of the interplay between tow components of our physical environment – water and earth. Porous pavement utilization attempts to sustain physical processes ongoing under natural conditions.“

Recycled Concrete Aggregate

General

The use of recycled concrete aggregate diverts waste material from landfills and reduces the need for mining raw materials. The excessive studies done on using recycled concrete aggregate in wet concrete mixes indicate very little to no loss of compressive strength. The major concerns of using recycled concrete aggregate are associated with structural concrete, none of which would apply in low traffic pervious pavement applications.

Recycled concrete has been used as aggregate in new concrete and as a base under pavement. Recycled concrete is simply a old crushed up pavement or structural concrete. The properties and performance of the new concrete depends on the quality and source of the original concrete prior to being recycled. (PCA 2009)

Preparation and Uses

All foreign objects such as asphalt, soils, glass, gypsum board, plaster, roofing material, and wood should be removed. After such materials have been removed, the aggregate can be crushed and prepared for further use.(PCA 2009, U.S Department of Transportation Federal Highway Administration 2009). Recycled concrete aggregate has been used in new concrete for pavements, shoulders, median barriers, sidewalks, curbs and gutters, and bridge foundations.

Properties

Unless made with extremely low quality concrete, the recycled concrete aggregate is about the same quality as natural aggregate. It is acceptable to use 100% of coarse recycled aggregate but no more the 10 to 20% of fine recycled aggregate. Recycled concrete aggregate is more porous and therefore has a higher absorption then conventional aggregate and should be SSD before batching. Chloride in recycled concrete can be a problem if steel reinforcing is being used. (ECCO 1999)

CHAPTER 3
RESEARCH METHODOLOGY

Phase I: Recycled Concrete Aggregate

Recycled Concrete Aggregate No. 57 and Crusher Run

Two types of recycled concrete aggregate, no. 57 and Crusher Run (no. 57 mixed with fines) were obtained from Florida Concrete Recycling, Inc. The standard Test for Sieve Analysis of Fine and Coarse Aggregate (ASTM C 136), the standard Test for Density, Specific Gravity and Absorption of Coarse Aggregate (ASTM C 127), and the standard Test for Unit Weight (ASTM C29) were performed. In addition, the water displacement test was conducted to confirm the density and specific gravity of the aggregate.

Recycled Concrete Aggregate No. 6, No. 7, and No. 8

Based on the sieve analysis results of aggregate no. 57 and the crusher run, it was decided to eliminate the crusher run, and to crush and sieve the aggregate no. 57 to obtain three smaller aggregate size distribution groups.

The recycled concrete aggregate no. 57 was transported to the FDOT materials lab for crushing and subsequently sieved out at the Department of Civil and Coastal Engineering at the University of Florida. The three final aggregate size groups used in this study were: a) number 6 (-3/4" to +3/8"), b) number 7(-1/2" to +No4), and c) number 8 (-3/8" to +No8). Sieve Analysis (ASTM C136), Density, Specific Gravity, Absorption (ASTM C127), and unit weight (ASTM C29) were determined for each group of aggregate. In addition, the water displacement test was conducted to confirm the density and specific gravity of the aggregate.

Phase II: Trial Mixes

Several small trial batches of pervious concrete made with recycled concrete aggregate were prepared to establish the most appropriate mix design for the actual pervious concrete specimens tested in Phase IV.

Trial mixes and sample cylinders were made with different aggregate sizes (-3/4, -3/4" to +No4, -1/2" to +No4, and -3/8" to +No4), aggregate to cement ratios (3.2 to 4.5), and water to cement ratios (0.3 to 0.6). Each trial sample was examined visually and under running water. The final selected mix design is listed in Table 3-1.:

Table 3-1. Pervious concrete mix design used in this study

	Ratio by mass
Aggregate to Portland cement (A/C)	4.5:1
Water to Portland cement (W/C)	0.3 – 0.33*
Mineral admixtures:	
Fly ash	20%
Blast furnace slag	40% and 50%

* All mixes were initially designed with 0.3 w/c ratio, mixed in the mixer for 3 minutes and let sit still for 3 minutes. The wet mix was then visually examined for the proper sheen. If the proper sheen was not achieved, water was added slowly until sheen appeared, thus increasing the w/c ratio.

Phase III: Compaction Methods

To study the difference in compressive strength, porosity, and permeability due to compaction, three different compaction methods were used: 1) rodding (ASTM C192); 2) vibration (Modified ASTM C192); and 3) customized standard proctor (Modified ASTM D 698).

Gear

All samples were cast in 6"x6" cardboard cylinder molds. To ease the filling and compaction processed, a 6"x2" stainless steel collar was temporally placed on top of the cylinder mold. A 6"x2" steel, 18.87 lb weight was used during compaction methods 2 and 3 (Figure 3-1). Other tools used during compaction were: a 3/8" diameter rod, a 75 Hz frequency vibrating table, and a 5.5 lb. Proctor hammer.

Figure 3-1. 6”x6” cardboard cylinder mold, 6”x2” stainless steel collar, 6”x2” steel (18.87 lb.) weight.

Compaction by Rodding

The wet mix was placed in the 6”x6” cylinder mold in three layers. Each layer was roded 25 times. The top of the cylinder was screeded with straight edge as even as possible.

Compaction by Vibration

The 6”x2” collar was placed on top of the 6”x6” cylinder before the pervious concrete mix was ready. The wet mix was then placed into the prepared cylinder mold so that it extended about 1” into the stainless steel collar. The 18.87 weight was placed on top of the wet mix, extending about 1” above the top of the collar. Set up like so, the filled cylinder, caller and the weight were all set on a vibrating table and vibrated until the weight became stagnant. For aggregate size no. 6 the weight became stagnant at about 10 seconds, for aggregate no. 7 in about 13 seconds, and for aggregate no. 8 in about 15 seconds.

Compaction by Customized Standard Proctor

The 6”x2” collar was placed on top of the 6”x6” cylinder before the pervious concrete mix was ready. The wet mix was then placed into the prepared cylinder mold so that it extended about 1” into the stainless steel collar. The weight was placed on top of the wet mix, extending

about 1" above the top of the collar. The standard Proctor 5.5lb hammer was dropped from 1ft height 75 times (equaling 412.5 ft-lb) on top of the weight. A cotton cloth was placed between the weight and the falling hammer to prevent damage to either tool.

NOTE: The Standard Proctor Test Method (ASTM D 698) was examined as one of the compaction methods. However, there were two major problems with this method. One was the damage caused to the aggregate by the direct impact of the 5.5 lb hammer (Figure 3-2). The second problem was due to the three-layer compaction, which disturbed the cement paste coating around the aggregate at the top of each layer, creating three potentially weak areas.

Figure 3-2. A trial sample showing aggregate (no. 6) damage caused by the direct impact of the 5.5 lb. Proctor hammer.

Phase IV: Mixing and Curing

Cementitious materials

The cementitious materials used in this study were Portland cement type II (Table 3-2), Fly Ash class F (Table 3-3), and Granulated Blast Furnace Slag (Table 3-4).

Table 3-2. Properties of portland cement type II

Blaine	Setting Time (min)		Compressive Strength (N/mm^2)						
(cm^2/g)	Initial	Final	3 days	7 days	Al_2O_3	Fe_2O_3	MgO	SO_3	LOI
2800	45	375	1450	2470	6.0	6.0	6.0	3.0	3

Table 3-3. Properties of Fly Ash class F

Specific gravity	Ig.loss	Moisture content	SiO2	Al2O3	Fe2O3	CaO	MgO	Na2O	SO3	K2O
2.18	2.32	0.07	57.9	26.79	4.45	2.44	0.94	0.54	0.28	2.41

Table 3-4. Properties of Granulated Blast Furnace Slag

Specific Gravity	Blaine (m2/kg)	Air Content (%)	S	SO_3
2.95	371	3.9	1.04	2.60

Sample Identification Labels

Twelve distinctive concrete mixes were designed. Three cylinders were poured from every mix; each compacted by one of the 3 different compaction methods, adding up to a total of 36 samples. The 36 pervious concrete samples break into the following specific categories:

- Three aggregate sizes: 1) No. 6, 2) No. 7, and 3) No. 8.
- Four different cementitious blends: 1) 100% Portland Cement, 2) 80% Portland Cement and 20% Fly Ash, 3) 50% Portland cement and 50% Slag, and 4) 40% Portland cement, 20% Fly Ash, and 40% Slag.
- Three different compaction methods: 1) rodding, 2) vibration, and 3) customized standard proctor .

A three-digit identification label was assigned to each sample. The first digit represents the aggregate size, the second digit represents the cementitious blend, and the third digit represents the compaction method. Table 3-5 shows the identification label matrix.

Table 3-5. Sample identification label matrix

Aggregate size →	No. 6 (1)			No. 7 (2)			No. 8 (3)		
Compaction method →	1	2	3	1	2	3	1	2	3
Plain Portland Cement (1)	111	112	113	211	212	213	311	312	313
20% Fly Ash (2)	121	122	123	221	222	223	321	322	323
50% Slag (3)	131	132	133	231	232	233	331	332	333
20% Fly Ash + 40% Slag (4)	141	142	143	241	242	243	341	342	343

Mixing Procedure

Prior to mixing, the concrete mixer was wetted and run empty a couple of times. The saturated surface dried (SSD) aggregate was weighed out and placed in the mixer. The mixer was turned on, and while mixing, all of the cementitious material was added, allowing it to coat each piece of aggregate. Next, all water was added. The mixer was left on for 3 minutes and then turned off for 3 minutes. During the sitting time the mix was visually inspected for metallic sheen. If the proper metallic sheen was not achieved with the initial water amount, more water was added. The mixer was then turned on for 2 more minutes.

Sample Curing

Immediately after mixing, the fresh concrete was placed into the prepared molds and compacted appropriately. The tops of all samples were covered with plastic wrap within 5 minutes of compaction. The cardboard molds were striped from the hardened samples after 24 ± 4 hours (tested for specific gravity, volume of voids, and porosity) and placed into a curing tank with saturated limewater. After 10 days, the samples were taken out of the curing tank and tested for permeability. The next day, the samples were sulfur capped at the materials research lab of the FDOT and let cure in air for 3 more days. On the 14^{th} day, samples were tested for compressive strength.

Phase V: Hardened Concrete Properties

A total of 36 samples were mixed, cured and tested. All samples were tested for Specific Gravity, Volume of Voids (cm^3), Porosity (%), Permeability (in/min.), and Compressive Strength (psi).

Specific Gravity, Volume of Voids (cm^3), Porosity (%)

The 24 ± 4 hours young concrete samples were weighed and their mass (Ms) was recorded in grams. Subsequently, the volume of solids (Vs) of each sample was determined by the water

displacement method. The water displaced by each sample (Vs) was weighed in grams (g = cm^3). Given that all samples were cast in 6" x 6" cylinder molds, the total volume (Vt) of 2780 cm^3 was assumed.

Equations 3-1 to 3-3 were used to calculate the desired properties:

$$\text{Specific Gravity} = \frac{Ms}{Vs} \tag{3-1}$$

$$\text{Volume of Voids (Vv)} = Vt - Vs \tag{3-2}$$

$$\text{Porosity} = \frac{Vv}{Vt} * 100 \tag{3-3}$$

Permeability (in/min)

A falling head permeameter was constructed to test the permeability of the pervious concrete samples (Figure 3-3). A large photo of the actual falling head permeameter was places in Appendix A. The permeameter was designed with a downward flow through the sample.

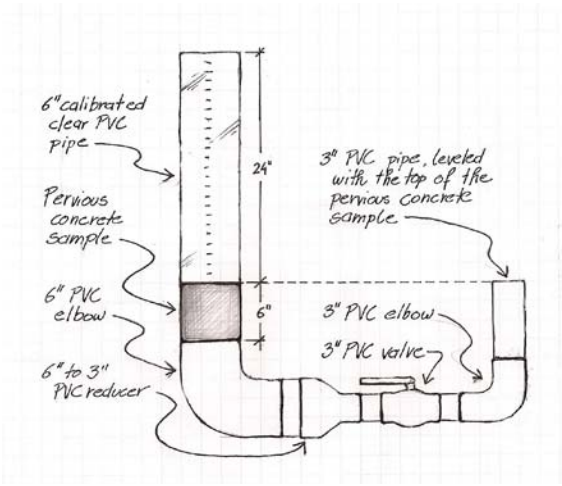

Figure 3-3. Sketch of the falling head permeameter

Before setting the samples into the permeameter, the samples were partially remolded. The remolded samples were set into the permeameter and secured with rubber gasket. The 6”

diameter, 24” long, calibrated clear stand pipe was securely placed on top of the sample using a second rubber gasket. The overflow pipe (on the opposite side of the permeameter) was then adjusted to be leveled with the top of the specimen / the 0” mark at the bottom of the calibrated clear cylinder.

With the valve in the open position, the entire system was filled with water to force out any air trapped in the pipes or the pervious concrete sample. Once equilibrium was reached (at 0”), the valve was closed. Next, the calibrated clear cylinder stand pipe was filled with water up to 22”. As the valve was opened, a stopwatch was started. The time (t) elapsed while the water head was falling from 22” (h_0) to 2” (h_1) was recorded.

The permeability coefficient (k) can be calculated according to Darcy’s law:

$$k = \frac{aL}{At} \ln \frac{h_0}{h_1} \tag{3-4}$$

Where

a = area of cross-section of standpipe (calibrated clear cylinder)

L = length of the pervious concrete sample

A = area of cross-section of the pervious concrete sample

t = the time elapsed while water head was falling from h_0 to h_1

h_0 = the initial water head height

h_1 = the final water head height

However, the permeameter was designed so the cross-section areas of the standpipe and the pervious concrete sample are equal. Then since a=A, the equation can be simplified to:

$$k = \frac{L}{t} \ln \frac{h_0}{h_1} \tag{3-5}$$

Further more, the equation was tailored specifically for the 6” long pervious concrete sample and the water head fall from h_0 = 22” to h_1 = 2” to:

$$k = \frac{14.4}{t} \quad (3\text{-}5)$$

The process of setting up and operation the falling head permeameter (Object 3-1) is depicted in the attached video. This video features Sarah Farmerie operating the falling head permeameter and was recorded by Kristyna T. Lannon.

Object 3-1. The process of setting up and operation the falling head permeameter (.AVI file289MB)

Compressive Strength (psi)

The compressive strength of the pervious concrete samples was tested with the “Tinius Olsen Super “L” hydraulic universal testing machine for critical materials testing up to 3,000 kN” (Figure 3-4). The machine was set up to a constant loading rate of 0.05 in/min.

Due to the uneven surface of the pervious concrete, the tops and bottoms of the samples were sulfur capped prior to testing for more accurate reading. Sulfur capping took place at the materials lab at the FDOT and allowed for more accurate compressive strength results.

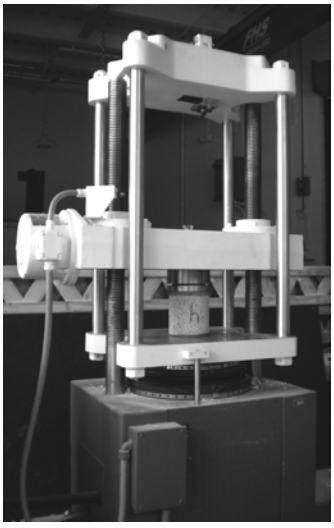

Figure 3-4. Tinius Olsen Super L hydraulic universal testing machine

CHAPTER 4
DATA ANALYSIS AND RESULTS

Aggregate Properties

Properties of Recycled Concrete Aggregate Size no. 57 and Crusher Run

Two sieve analyses were carried out on the recycled concrete aggregate no. 57, and the Crusher Run aggregate (no. 57 mixed with fines) as delivered from the Florida Concrete Recycling, Inc. to determine the aggregate size distribution and to evaluate the need for further crushing and sieving. The results summary tables and the aggregate size distribution graphs of the sieve analysis #1 and sieve analysis #2 can be found in Appendixes B and C, respectively.

The sieve analysis for the Crusher Run aggregate resulted in 82% passing sieve no. 4 and 64-66% passing sieve no. 8. Such large amount of fines was unfit for this study. The Crusher Run aggregate was therefore not used and was eliminated from further testing.

The sieve analysis for aggregate no. 57 resulted in 44 to 47% retained on the 1" sieve, 69 to 81% not passing the 3/4" sieve, and 88 to 95% not passing the 1/2" sieve.

The specific gravity, density, and absorption (ASTM C127) and unit weight (ASTM C29) tests were conducted along with the water displacement test were conducted for aggregate no. 57. The results are summarized in Table 4-1.

Table 4-1. Properties of aggregate size no. 57

	Aggregate size no. 57
Specific Gravity – OD	2.12
Specific Gravity – SSD using ASTM C127	2.27
Specific Gravity – SSD using water displacement method	2.24
Apparent Specific Gravity	2.48
Density – OD (lb/ft^3)	132.23
Density – SSD using ASTM C127 (lb/ft^3)	141.40
Density – SSD using water displacement method (lb/ft^3)	139.84
Apparent Density (lb/ft^3)	155.97
Absorption (%)	6.96
Unit weight (lb/ft^3)	80

Properties of Recycled Concrete Aggregate no. 6, 7, and 8

It was decided that smaller size aggregate than the no. 57 was needed. The recycled concrete aggregate no. 57 was run through an aggregate crusher at the FDOT materials research lab. Due to the limited adjustability of the crusher and the aggregate's soft nature, the crushing resulted in a significant amount of fines and 3/8" pieces. The second most common aggregate size in the crushed pile was 1/2".

Post crushing, the material was combined with the original no. 57 aggregate and three aggregate size distribution groups according to the ASTM C33: a) no. 6 (-3/4" to +3/8"), b) no. 7 (-1/2" to +No4), and c) no.8 (-3/8" to +No8) were sieved out. Once the needed amount of aggregate was acquired, each group was subjected to proper sieve analysis. The results of each sieve analysis and the size distribution graphs can be found in Appendix D.

The aggregates were tested per ASTM C127 for specific gravity, density, and absorption, and per ASTM C29 for unit weight. The specific gravity and density were also tested using the water displacement method. These results are summarized in Table 4-2.

Table 4-2. Properties of aggregate no. 6, no. 7, and no. 8

	Aggregate size no. 6	Aggregate size no. 7	Aggregate size no. 8
Specific gravity - OD	2.12	2.14	2.16
Specific gravity - SSD using ASTM C127	2.25	2.26	2.29
Specific gravity - SSD using water displacement method	?2.36?	?2.12?	?2.13?
Apparent specific gravity	2.44	2.45	2.48
Density - OD	132.35	133.14	134.72
Density- SSD using ASTM C127	140.59	141.34	142.78
Density - SSD using water displacement method	?147.34?	?132.35?	?132.98?
Apparent density	152.45	152.83	154.76
Absorption	6.2	5.9	6
Unit weight	83.4	85.2	85.0

Pervious Concrete Mix Design

All twelve concrete batches were designed and weighed out with an A/C ratio of 4.5:1 and W/C ratio of 0.3 and predetermined percentage of FA and GBFS. When needed, extra water was added to each individual batch during mixing until the desired sheen was achieved. The actual W/C ratio of each batch was then determined depending on the amount of extra water added. Table 4-3 lists the final mix design of each batch.

Table 4-3. Final mix design

ID no.	PC	Fly ash	Slag	a/c	w/c
111, 112, 113	100%	-	-	4.5:1	0.31
121, 122, 123	80%	20%	-	4.5:1	0.31
131, 132, 133	50%	-	50%	4.5:1	0.33
141, 142, 143	40%	20%	40%	4.5:1	0.32
211, 212, 213	100%	-	-	4.5:1	0.32
221, 222, 223	80%	20%	-	4.5:1	0.32
231, 232, 233	50%	-	50%	4.5:1	0.32
241, 242, 243	40%	20%	40%	4.5:1	0.32
311, 312, 313	100%	-	-	4.5:1	0.30
321, 322, 323	80%	20%	-	4.5:1	0.30
331, 332, 333	50%	-	50%	4.5:1	0.31
341, 342, 343	40%	20%	40%	4.5:1	0.30

Properties of Pervious Concrete Samples

Specific Gravity, Volume of Voids, Porosity

From the specific gravity, volume of voids, and porosity test, it is the porosity results, which are most important to this study. As shown in Table 4-4, porosity decreased as the aggregate size decreased, and was consistently lowest in samples compacted by rodding. The most variety in porosity was realized in samples compacted by vibration. The porosity was also decreased in over 65% of the samples containing Fly Ash. The relationship between A) porosity and compaction, and B) porosity and cementitious blends for each sample is graphed in Figure 4-1. Figure 4-2 is a break down of Figure 4-1A. It consists of three graphs depiction porosity vs. only one compaction method per graph.

Table 4-4. Specific gravity, volume of voids, and porosity of all 36 samples

ID no.	SG	Vv (cm^3)	Porosity (%)	ID no.	SG	Vv (cm^3)	Porosity (%)	ID no.	SG	Vv (cm^3)	Porosity (%)
111	2.25	735	26.44	211	2.22	761	27.37	311	2.14	703	25.29
112	2.28	970	34.89	212	2.22	836	30.07	312	2.11	810	29.14
113	2.32	975	35.07	213	2.30	898	32.30	313	2.18	784	28.20
121	2.21	705	25.36	221	2.22	710	25.54	321	2.15	670	24.10
122	2.25	888	31.94	222	2.26	884	31.80	322	2.15	778	27.99
123	2.26	903	32.48	223	2.18	829	29.82	323	2.22	805	28.96
131	2.28	738	26.55	231	2.27	757	27.23	331	2.16	690	24.82
132	2.23	838	30.14	232	2.19	840	30.22	332	2.14	738	26.55
133	2.35	958	34.46	233	2.13	765	27.52	333	2.13	800	28.78
141	2.23	750	26.98	241	2.23	753	27.09	341	2.10	647	23.27
142	2.27	930	33.45	242	2.17	790	28.42	342	2.07	674	24.24
143	2.25	899	32.34	243	2.27	890	32.01	343	2.20	773	27.81

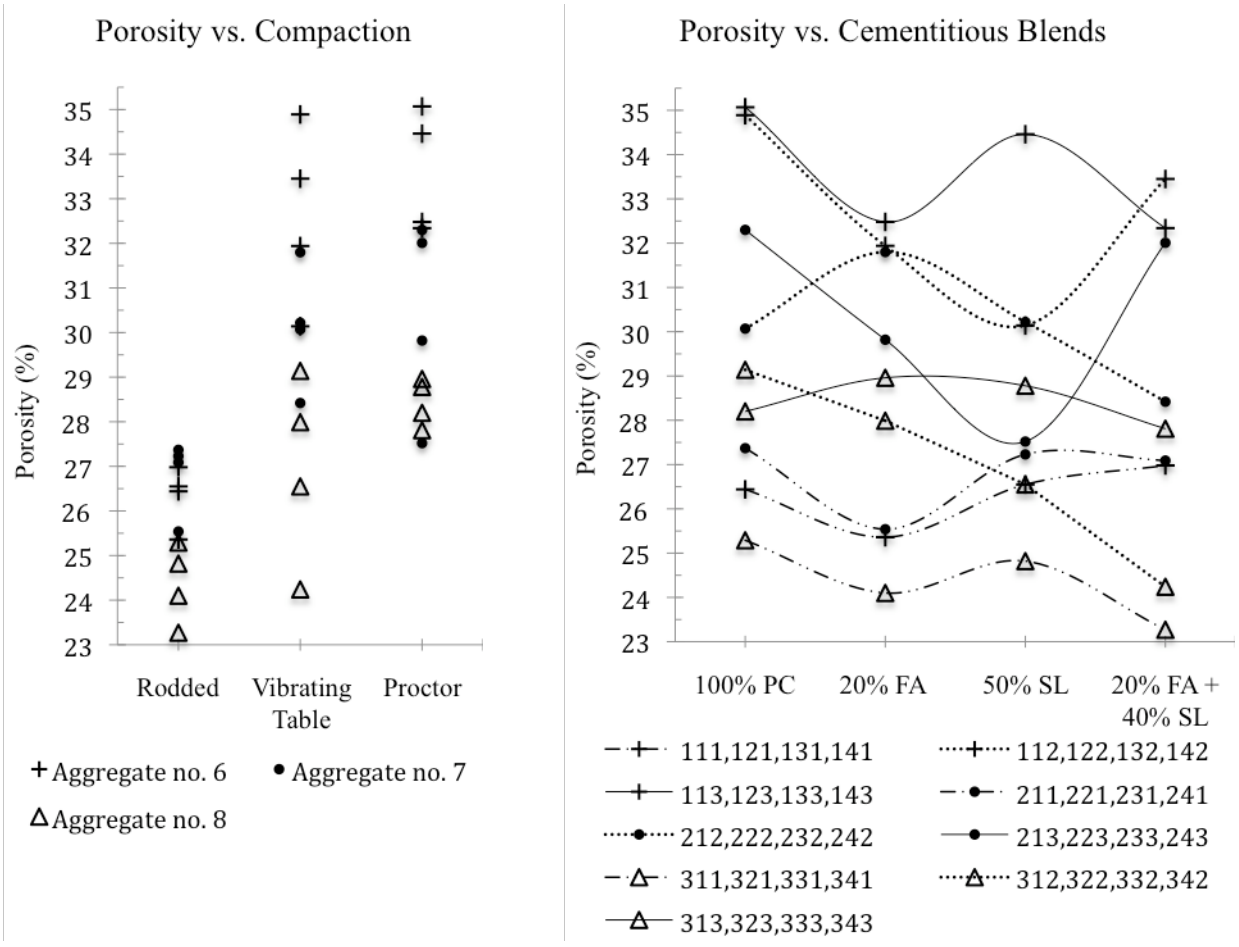

A B

Figure 4-1. A) Graph showing the relationship between porosity and compaction for all samples B) Graph showing the relationship between porosity and cementitious blends for all samples

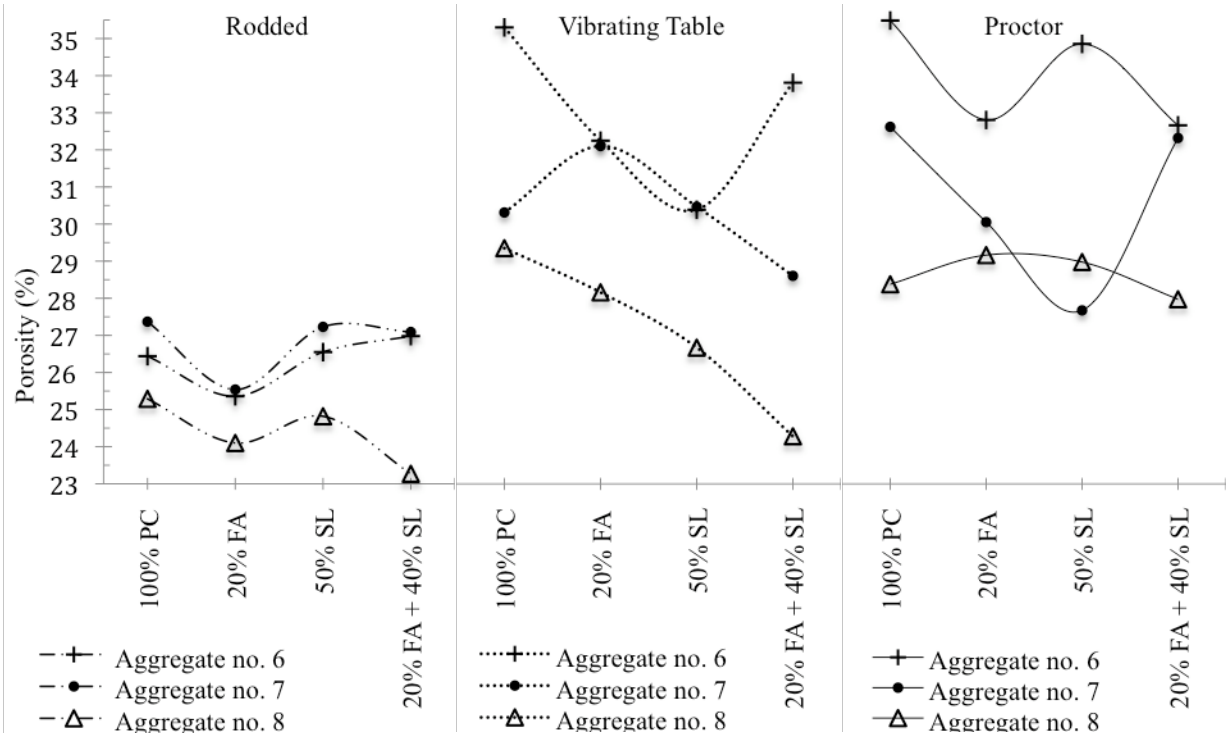

A B C

Figure 4-2. A) Graph showing the relationship between porosity and cementitious blends for samples compacted by rodding B) Graph showing the relationship between porosity and cementitious blends for samples compacted by vibration C) Graph showing the relationship between porosity and cementitious blends for samples compacted by customized proctor method

Permeability

Per the results listed in Table 4-5, permeability rates from 0.5 to 1.9 in/s (30 to 114 in/min.) were realized. The permeability ranges are consistently lower for samples made with aggregate no 8 and samples compacted by rodding. For most parts, permeability shows similar patterns to porosity in relationship to compaction methods. However, unlike porosity, the permeability rates tend to be lower in samples made with 50% blast furnace slag compared to the once made with 100% Portland cement and 20% Fly Ash. The relationship between A) permeability and compaction, and B) permeability and cementitious blends for all sample are

graphed in Figure 4-3. Figure 4-4 is a break down of Figure 4-3A. It consists of three graphs depiction permeability vs. only one compaction method per graph.

Table 4-5. Permeability of all 36 samples

ID no.	Permeability (in/s)	ID no.	Permeability (in/s)	ID no.	Permeability (in/s)
111	1.1	211	0.9	311	0.7
112	1.8	212	1.0	312	1.0
113	1.9	213	1.2	313	0.9
121	1.2	221	0.8	321	0.6
122	1.5	222	1.2	322	0.9
123	1.7	223	1.3	323	0.8
131	0.8	231	0.9	331	0.6
132	1.3	232	1.2	332	1.0
133	1.4	233	1.2	333	0.7
141	1.2	241	0.9	341	0.5
142	1.5	242	1.0	342	0.6
143	1.6	243	1.2	343	0.6

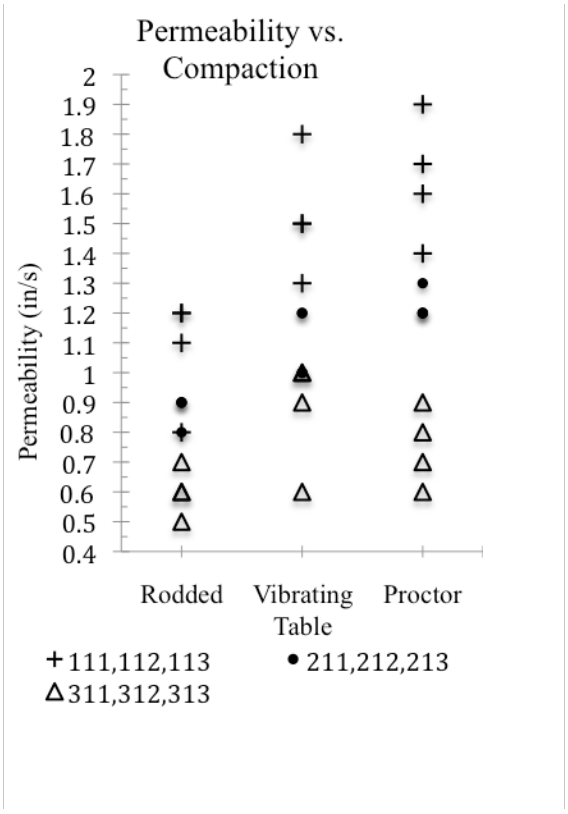

A

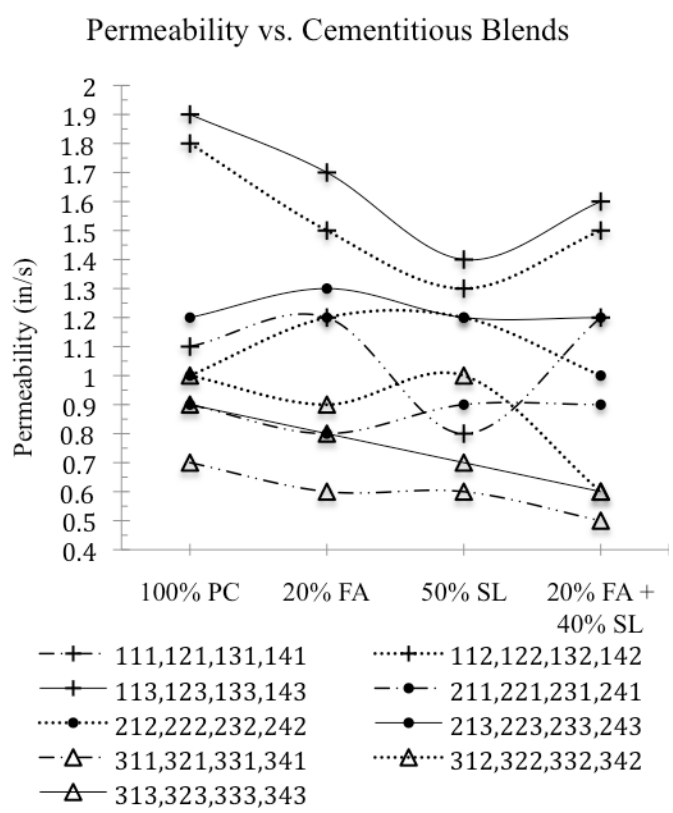

B

Figure 4-3. A) Graph showing the relationship between permeability and compaction for all samples B) Graph showing the relationship between permeability and cementitious blends for all samples

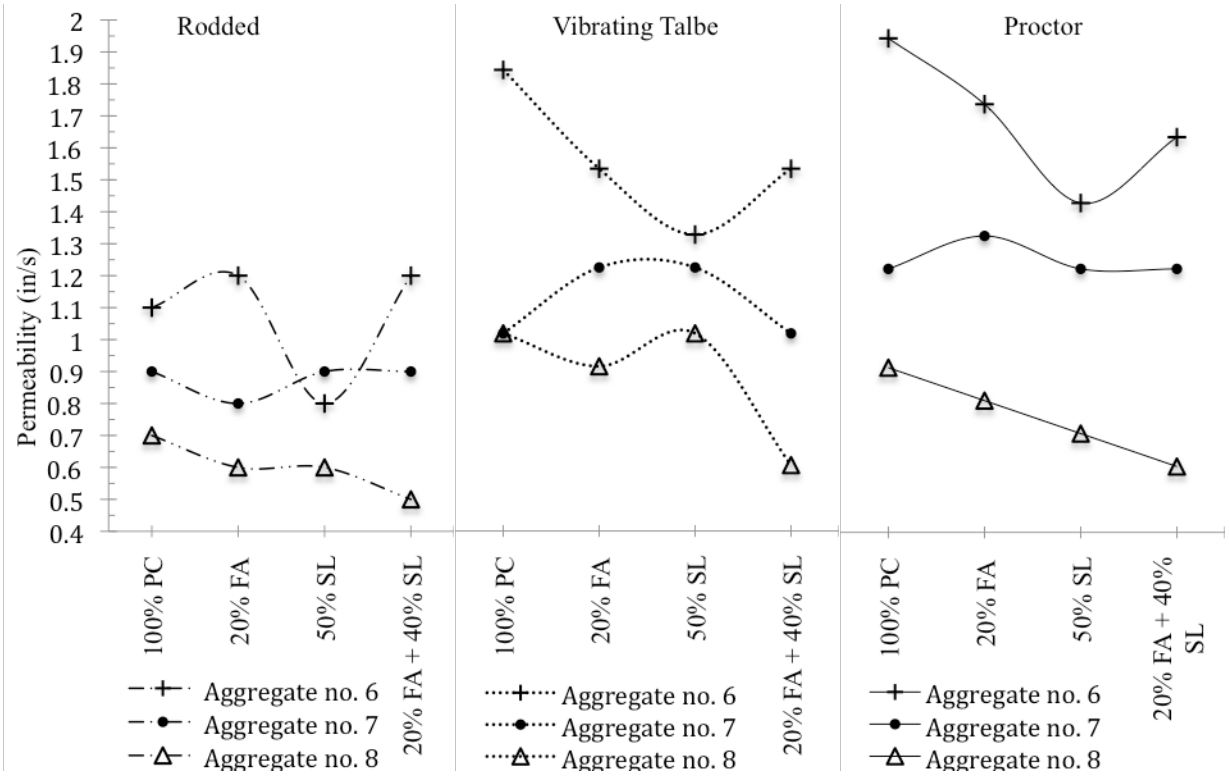

Figure 4-4. A) Graph showing the relationship between permeability and cementitious blends for samples compacted by rodding B) Graph showing the relationship between permeability and cementitious blends for samples compacted by vibration C) Graph showing the relationship between permeability and cementitious blends for samples compacted by customized proctor method

Compressive Strength

The compressive strength results are listed in Table 4-6. The highest adjusted compressive strength of 1330 psi was achieved for sample 231 and the lowers adjusted psi of 627 was realized in sample 312. In general the compressive strength was higher for samples made with no 6 aggregate and those compacted by rodding. The results also indicate that samples with 50% blast furnace slag have more compressive strength. The relationship between compressive strength and compaction, and compressive strength and cementitious blends for each sample was graphed in Figure 4-5. Figure 4-6 is a break down of Figure 4-5A. It consists of three graphs depiction compressive strength vs. only one compaction method per graph.

Table 4-6. Compressive Strength of all 36 samples

ID no.	CS (psi)	Adjusted* CS (psi)	ID no.	CS (psi)	Adjusted* CS (psi)	ID no.	CS (psi)	Adjusted* CS (psi)
111	1523	1325	211	1251	1088	311	1241	1080
112	897	780	212	1109	965	312	721	627
113	769	669	213	968	842	313	885	770
121	1388	1208	221	1327	1154	321	1306	1136
122	1083	942	222	1043	907	322	985	857
123	855	744	223	900	783	323	866	753
131	1496	1302	231	1529	1330	331	1301	1132
132	1226	1067	232	1124	978	332	973	847
133	868	755	233	1011	880	333	-	-
141	1325	1153	241	1217	1059	341	1086	945
142	886	771	242	1178	1025	342	1046	910
143	860	748	243	886	771	343	903	786

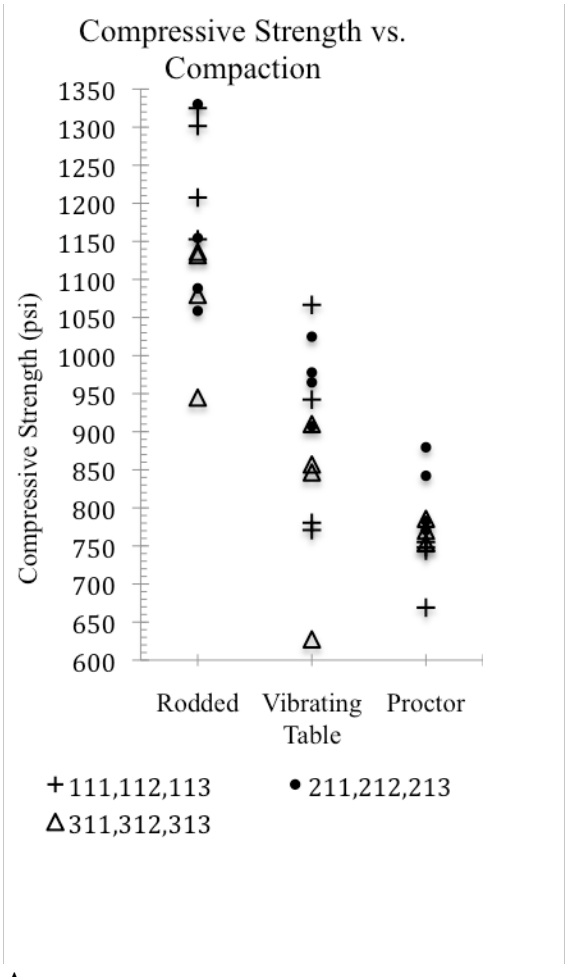

A

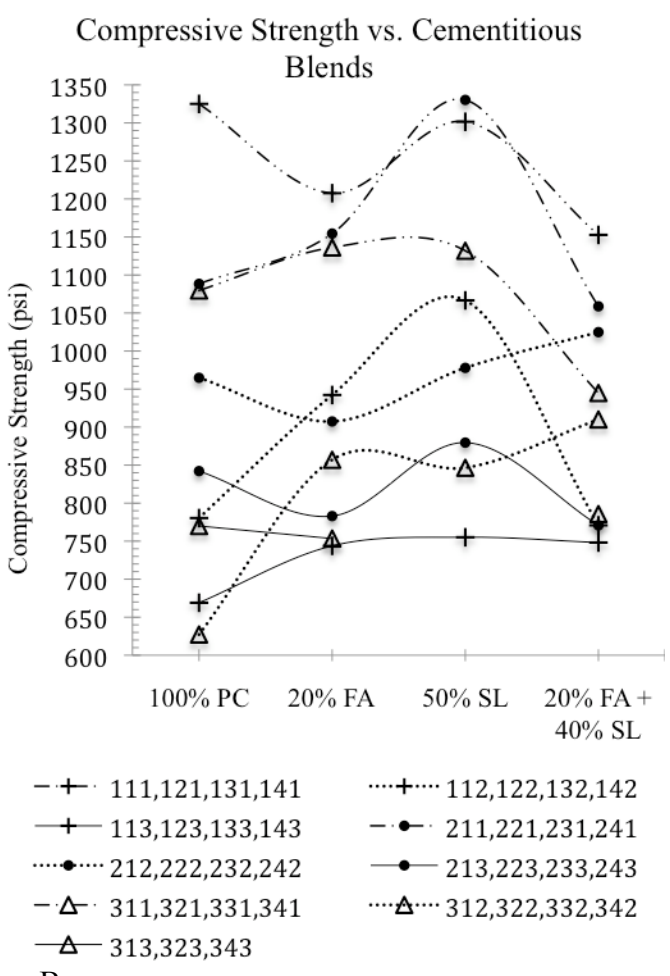

B

Figure 4-5. A) Graph showing the relationship between compressive strength and compaction for all samples B) Graph showing the relationship between compressive strength and cementitious blends for all samples

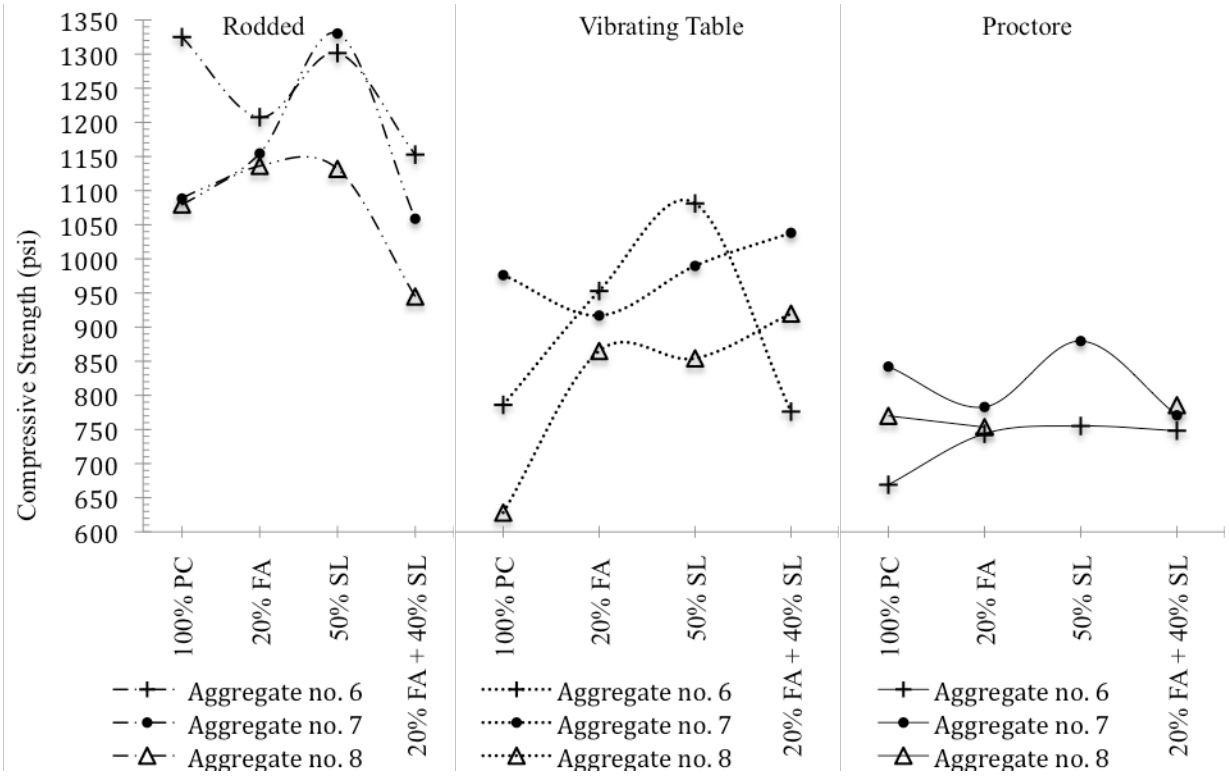

Figure 4-6. A) Graph showing the relationship between compressive strength and cementitious blends for samples compacted by rodding B) Graph showing the relationship between compressive strength and cementitious blends for samples compacted by vibration C) Graph showing the relationship between compressive strength and cementitious blends for samples compacted by customized proctor method

The compressive strength was graphed against permeability in Figure 4-7. This figure shows a strong pattern in terms of aggregate size. A linear trendline was drawn for samples made with the same aggregate size resulting in R^2 of 0.81 for aggregate no 6, 0.72 for aggregate no 7, and 0.39 for aggregate no. 8.

The hydraulic universal testing machine use in this study plotted the compressive strength (psi) vs. the time (s). These graphs along with a photo of the appropriate crushed sample are included in Appendix E.

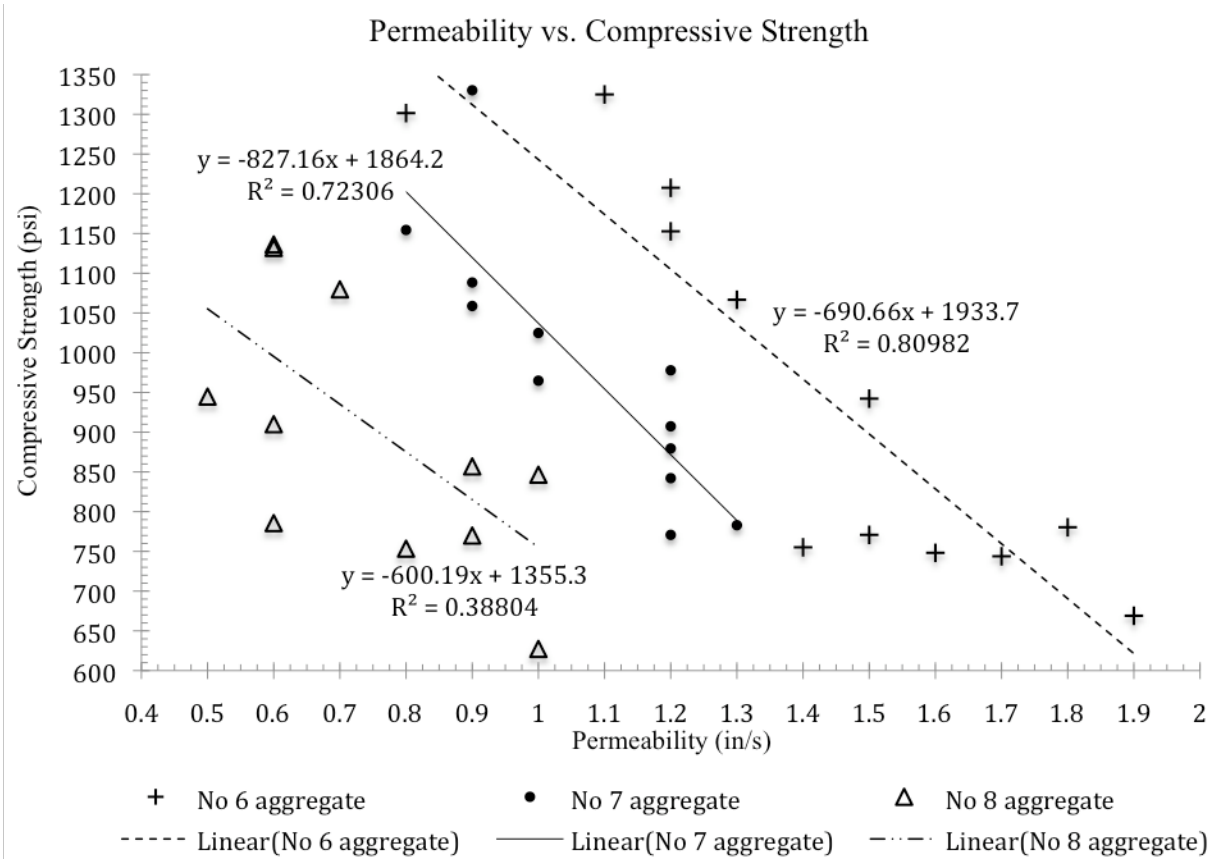

Figure 4-7. A) Graph showing the relationship between permeability and compressive strength for all samples

CHAPTER 5
CONCLUSION

General

In conclusion, it can be said that 100% of recycled concrete aggregate and up to 60% of mineral admixtures can be successfully used in the production of pervious concrete to reduce the environmental impact of the final product. The pervious concrete properties gathered in this study in terms of aggregate size, compaction, and compressive strength are discussed below.

Aggregate Size

The aggregate size made a significant difference in the pervious concrete samples' porosity, permeability and compressive strength. The porosity and permeability both increase with the aggregate size. This is consistent with previous research conducted on pervious concrete made with virgin aggregate. However, contradictory to pervious research (Crouch et al. 2007), the highest compressive strength was found in samples made with no. 6 aggregate, which was the largest aggregate used. This could be that the same A/C ratio of 4.5:1 was used for all samples, so the larger aggregate samples had thicker coating around each peace of aggregate, creating a stronger bond.

Compaction

Surprisingly, compaction by rodding produced the strongest samples of all three compaction methods. This is believed to be due to the three-layer compaction. During the customized proctor method the wet mix was compacted by 412.5 ft-lb force with 18.87 lb weight, but only in one layer. This consolidation method resulted in less overall compaction. The vibration method seamed to effect the migration of the paste more so then aggregate compaction. As can be seen in Appendixes F, G, H, which show the bottom views of all samples, the samples compacted by vibration have the most settled paste.

Compressive Strength

Compared to pervious concrete made with virgin aggregate, no significant reduction in compressive strength was realized by replacing the aggregate by recycled concrete. The somewhat low compressive strength results achieved in this study can be contributed to the short curing time of 14 days and the low compaction energies used. The effect of the aggregate size on compressive strength is discussed are the "Aggregate Size" section of this chapter.

CHAPTER 6
RECOMMENDATIONS

Design mix

The A/C and W/C ratios for this study were limited to 4.5:1 and 0.30 - 0.32 respectively. The resulted high permeability and the low compressive strength suggest that higher A/C ratio or even a small amount of fine aggregate could be used to increase the compressive strength while sustaining adequate permeability rate.

Compaction

The compaction levels used in this study were fairly low and more compaction force could be applied to achieve higher compressive strength. Some possible compaction techniques recommended are combination of rodding and vibration and using the modified proctor 10 lb hammer in the customized proctor method.

Field Study

There is a significant difference between results obtained in the lab and the way pervious concrete pavement would actually perform in the field. Therefore, a field study of pervious concrete pavement made with recycled concrete aggregate is recommended.

APPENDIX A
FALLING HEAD PERMEAMETER

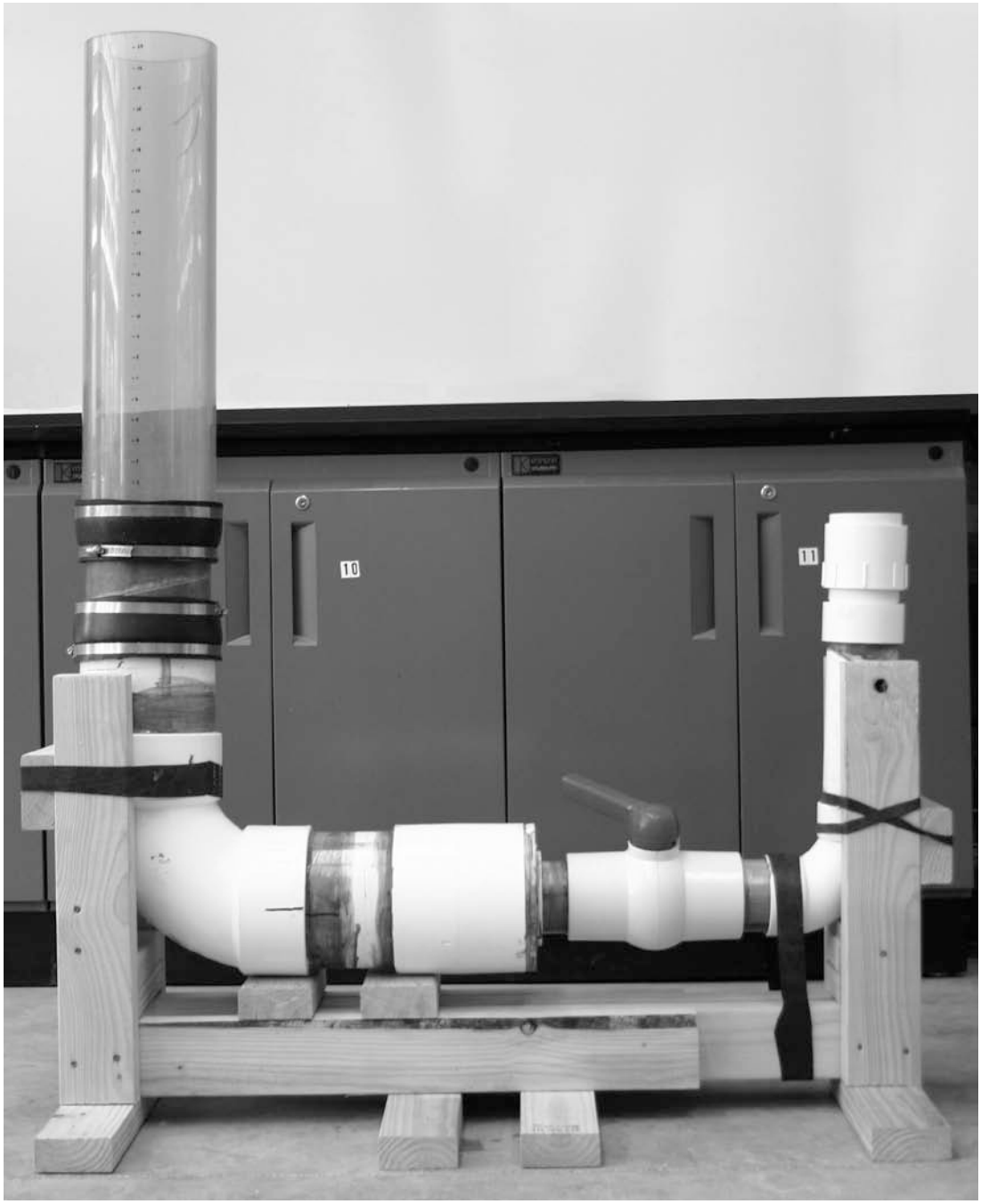

Figure A-1. Permeameter built by Kristyna T Lannon and Sarah Farmerie from parts donated by WW Gay mechanical contractor and with the support of Dr. Issa.

APPENDIX B
RESULTS OF THE SIEVE ANLYSIS #1 OF RECYCLED CONCRETE AGGREGATE NO. 57 AND CRUSHER RUN AS DELIVERED FROM THE FLORIDA CONCRETE RECYCLING, INC.

Table B-1. Aggregate no. 57: Sieve Analysis #1, Sample Size: 2,363g

Sieve #	Mass of Each Sieve (g)	Mass of Each Sieve + Retained Aggregate (g)	Mass of Retained Aggregate (g)	% Retained	Cumulative % Retained	% Passing
1 1/2 in	513	513	0	0.00	0	100.00
1 in	547	1597	1050	44.42	44.42	55.58
3/4 in	551	1121	570	24.11	68.53	31.47
1/2 in	551	1019	468	19.80	88.32	11.68
3/8 in	766	892	126	5.33	93.65	6.35
4 (0.187 in)	748	806	58	2.45	96.11	3.89
Pan	518	610	92	3.89	100.00	0
Total	3681	6558	2364	100		

Table B-2. Crusher Run (no. 57 mixed with fines): Sieve Analysis #1, Sample Size: 1,055g

Sieve #	Mass of Each Sieve (g)	Mass of Each Sieve + Retained Aggregate (g)	Mass of Retained Aggregate (g)	% Retained	Cumulative % Retained	% Passing
4 (0.187 in)	747	932	185	17.54	17.52	82.48
8 (0.0937 in)	680	857	177	16.78	34.31	65.69
16 (0.0469 in)	423	577	154	14.60	48.91	51.09
30 (0.0234 in)	305	462	157	14.88	63.79	36.21
50 (0.0117 in)	279	440	161	15.26	79.05	20.95
100 (0.0059 in)	261	381	120	11.37	90.43	9.57
Pan	518	619	101	9.57	100.00	0
Fineness Modulus:					3.34	
Total	2466	4268	1055	100		

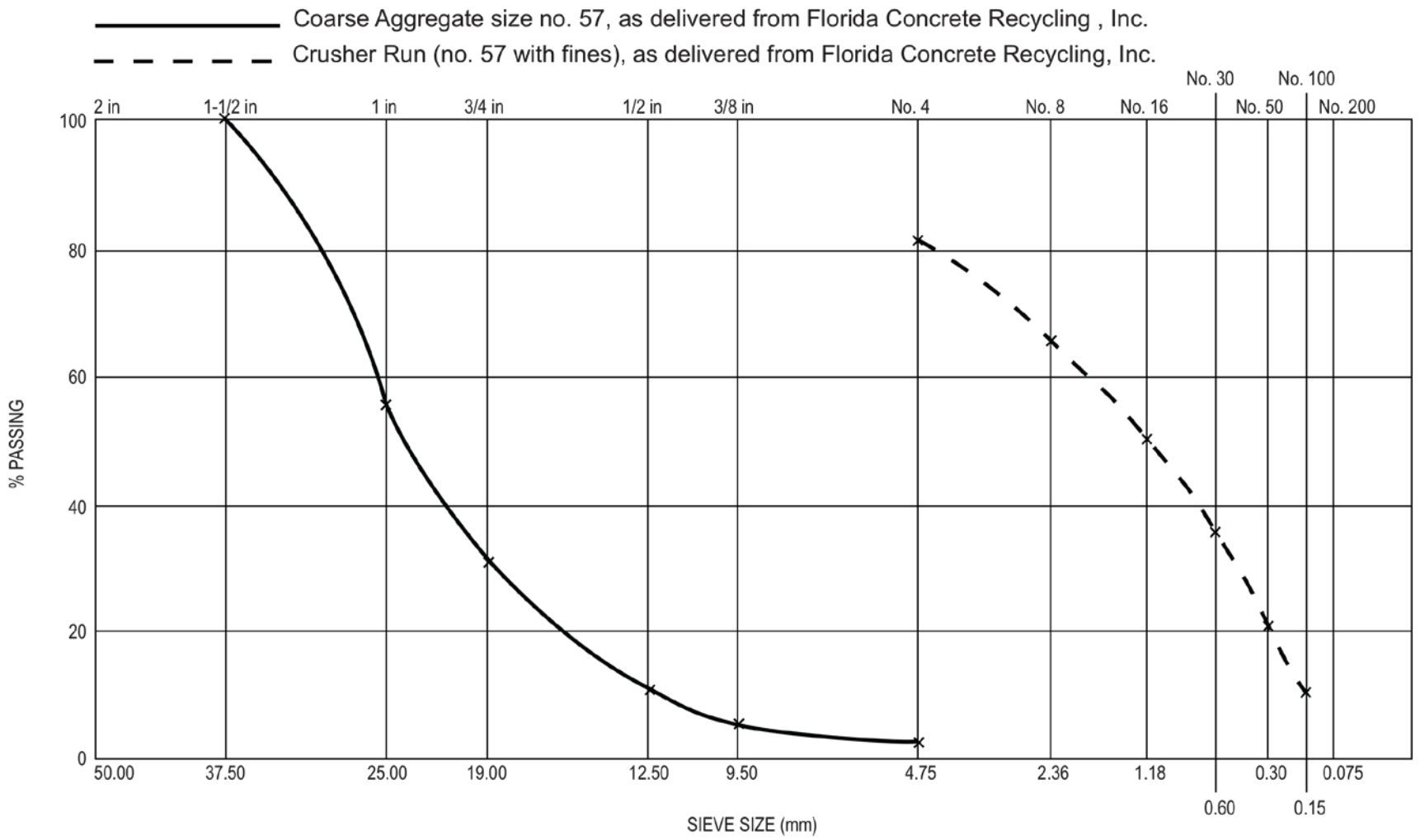

Figure B-1. Aggregate size distribution graph #1 for coarse aggregate no. 57 and crusher run (no. 57 with fines)

APPENDIX C
RESULTS OF THE SIEVE ANLYSIS #2 OF RECYCLED CONCRETE AGGREGATE NO. 57 AND CRUSHER RUN AS DELIVERED FROM THE FLORIDA CONCRETE RECYCLING, INC.

Table C-1. Aggregate no. 57: Sieve Analysis #2, Sample Size: 2,564g

Sieve #	Mass of Each Sieve (g)	Mass of Each Sieve + Retained Aggregate (g)	Mass of Retained Aggregate (g)	% Retained	Cumulative % Retained	% Passing
1 1/2 in	513	513	0	0.00	0	100.00
1 in	547	1741	1194	46.55	46.55	53.45
3/4 in	551	1432	881	34.35	80.90	19.10
1/2 in	551	924	373	14.54	95.44	4.56
3/8 in	766	845	79	3.08	98.52	1.48
4 (0.187 in)	748	759	11	0.43	98.95	1.05
Pan	518	545	27	1.05	100.00	0
Total	4194	6759	2565	100		

Table C-2. Crusher Run (no. 57 mixed with fines): Sieve Analysis #2, Sample Size: 1,055g

Sieve #	Mass of Each Sieve (g)	Mass of Each Sieve + Retained Aggregate (g)	Mass of Retained Aggregate (g)	% Retained	Cumulative % Retained	% Passing
4 (0.187 in)	747	937	190	18.01	18.01	81.99
8 (0.0937 in)	680	871	191	18.10	36.11	63.89
16 (0.0469 in)	423	583	160	15.17	51.28	48.72
30 (0.0234 in)	305	458	153	14.50	65.78	34.22
50 (0.0117 in)	279	434	155	14.69	80.47	19.53
100 (0.0059 in)	261	372	111	10.52	91.00	9.00
Pan	518	613	95	9.00	100.00	0
Fineness Modulus:					3.43	
Total	3213	4268	1055	100		

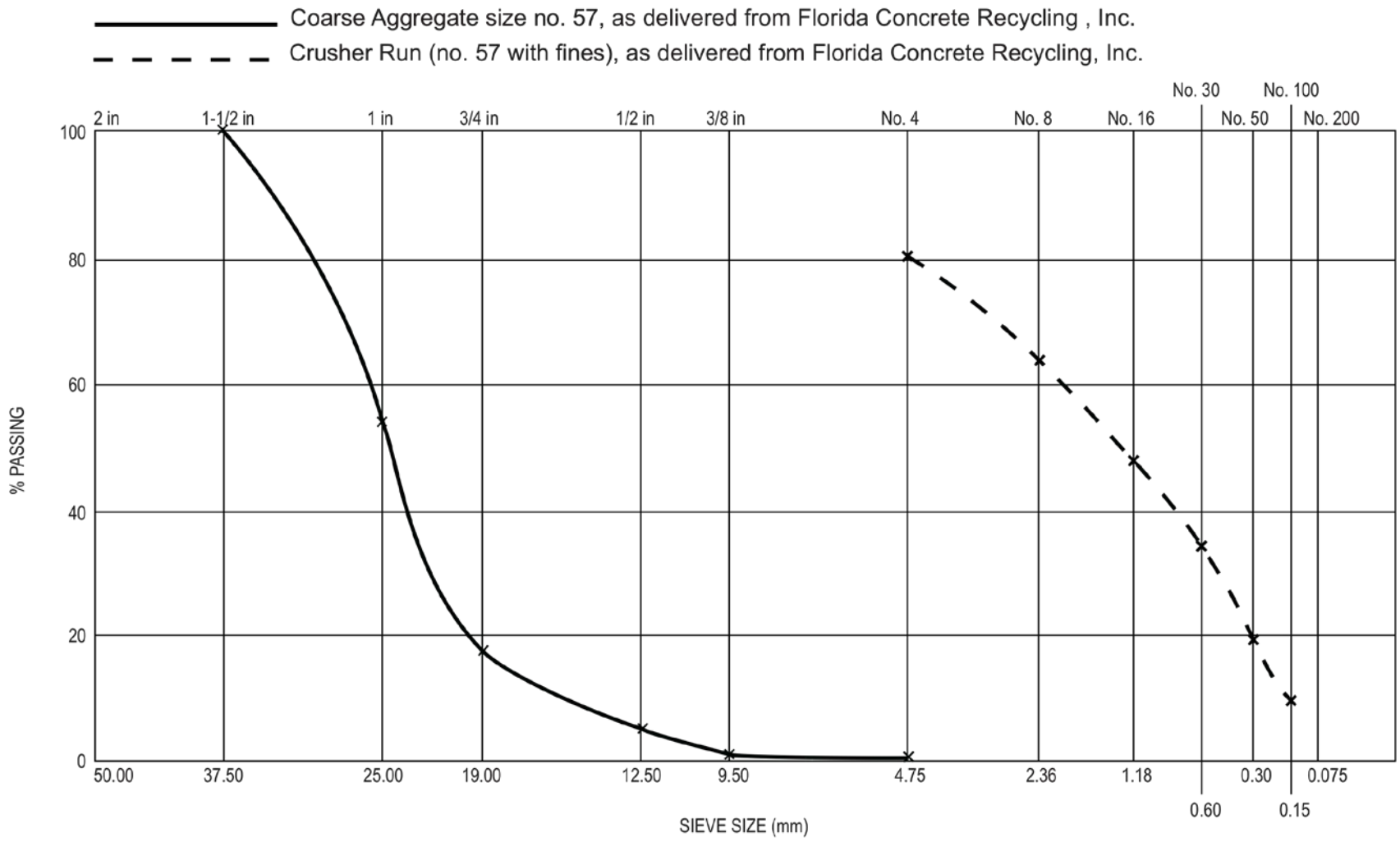

Figure C-1. Aggregate size distribution graph #2 for coarse aggregate no. 57 and crusher run (no. 57 plus fines).

APPENDIX D
SIEVE ANLYSIS OF RECYCLED CONCRETE AGGREGATES SIZE NO. 6, 7 AND 8

Table D-1. Aggregate no. 6, Sample Size: 1,100g

Sieve #	Mass of Each Sieve (g)	Mass of Each Sieve + Retained Aggregate (g)	Mass of Retained Aggregate (g)	% Retained	Cumulative % Retained	% Passing
3/4 in	551	551	0	0.00	0.00	100.00
1/2 in	552	1061	509	46.27	46.27	53.73
3/8 in	766	1219	453	41.18	87.45	12.55
4 (0.187 in)	592	709	117	10.64	98.09	1.91
8 (0.??? in)	577	581	4	0.36	98.45	1.55
16 (0.??? in)	425	425	0	0.00	98.45	1.55
Pan	519	536	17	1.55	100.00	0.00
Total	3982	5082	1100	100		

Table D-2. Aggregate no. 7, Sample Size: 1,000g

Sieve #	Mass of Each Sieve (g)	Mass of Each Sieve + Retained Aggregate (g)	Mass of Retained Aggregate (g)	% Retained	Cumulative % Retained	% Passing
1/2 in	552	552	0	0.00	0.00	100.00
3/8 in	766	1409	643	64.30	64.30	35.70
4 (0.187 in)	591	928	337	33.70	98.00	2.00
8 (0.??? in)	577	582	5	0.50	98.50	1.50
16 (0.??? in)	424	425	1	0.10	98.60	1.40
Pan	519	533	14	1.40	100.00	0.00
Total	3429	4429	1000	100		

Table D-3. Aggregate no. 7, Sample Size: 1,000g

Sieve #	Mass of Each Sieve (g)	Mass of Each Sieve + Retained Aggregate (g)	Mass of Retained Aggregate (g)	% Retained	Cumulative % Retained	% Passing
1/2 in	552	552	0	0.00	0.00	100.00
3/8 in	766	776	10	1.00	1.00	99.00
4 (0.187 in)	592	1484	892	89.20	90.20	9.80
8 (0.??? in)	579	659	80	8.00	98.20	1.80
16 (0.??? in)	425	427	2	0.20	98.40	1.60
Pan	518	534	16	1.60	100.00	0.00
Total	2880	3880	1000	100		

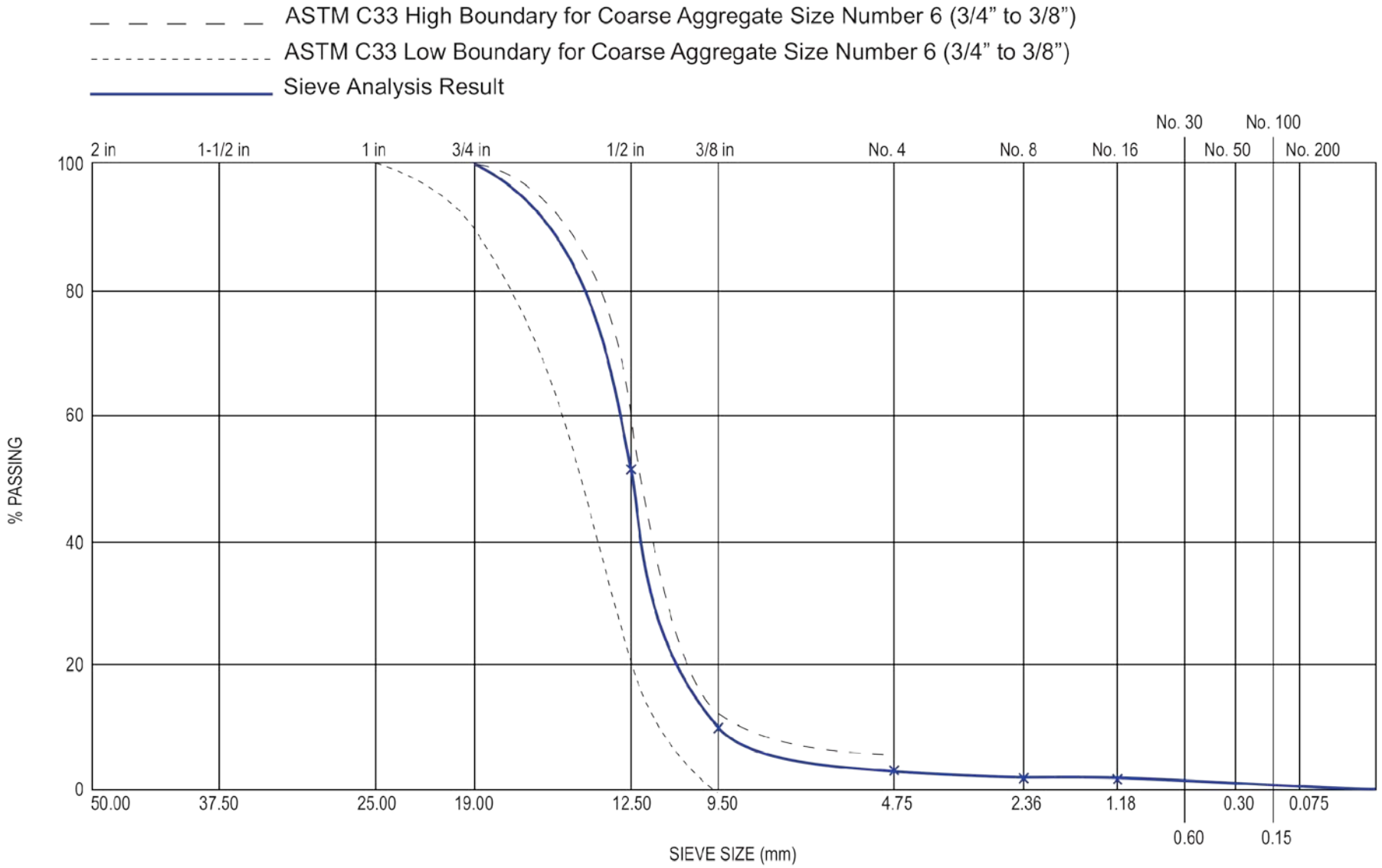

Figure D-1. Aggregate size distribution graph for coarse aggregate no. 6.

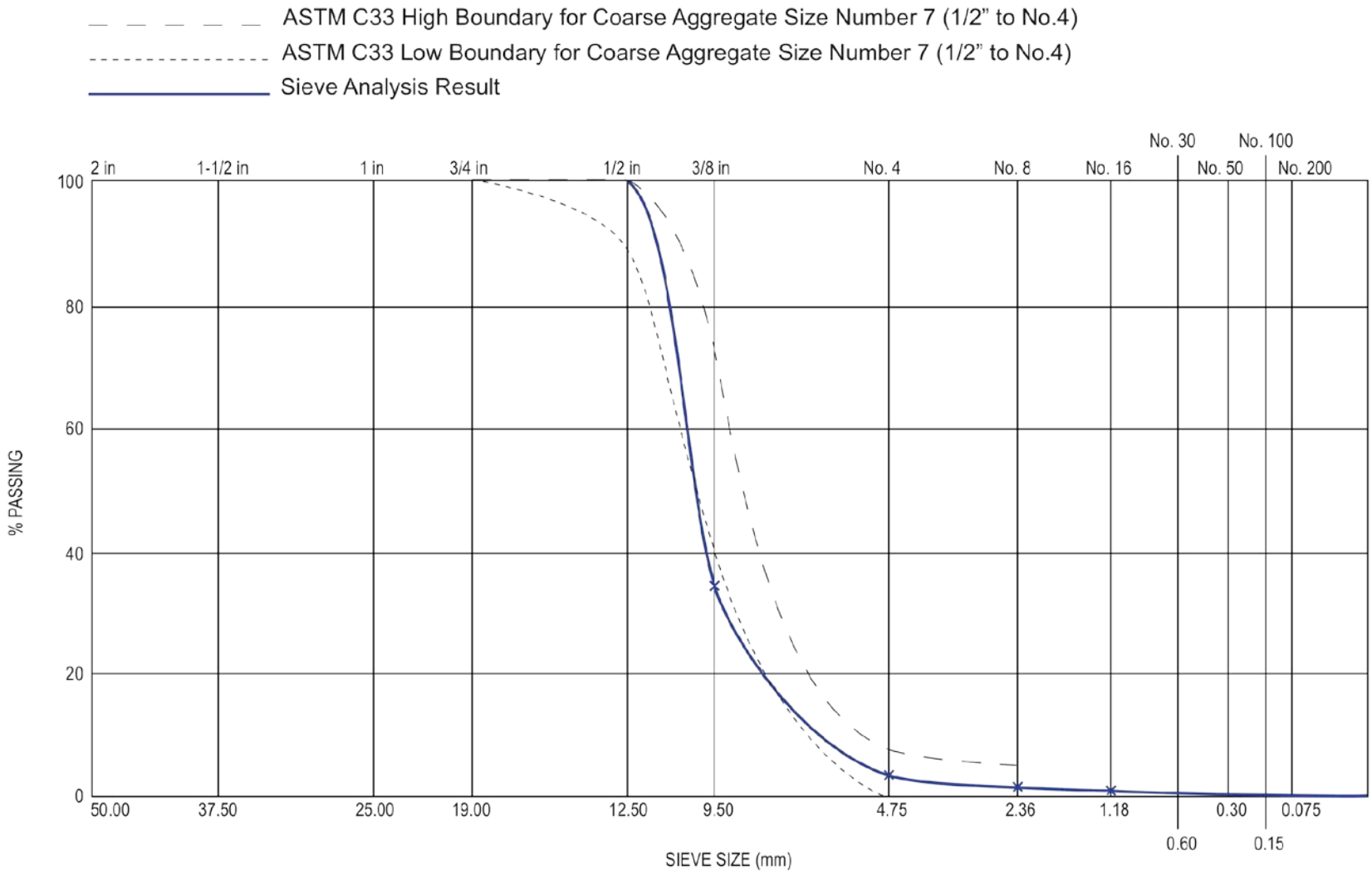

Figure D-2. Aggregate size distribution graph for coarse aggregate no. 7

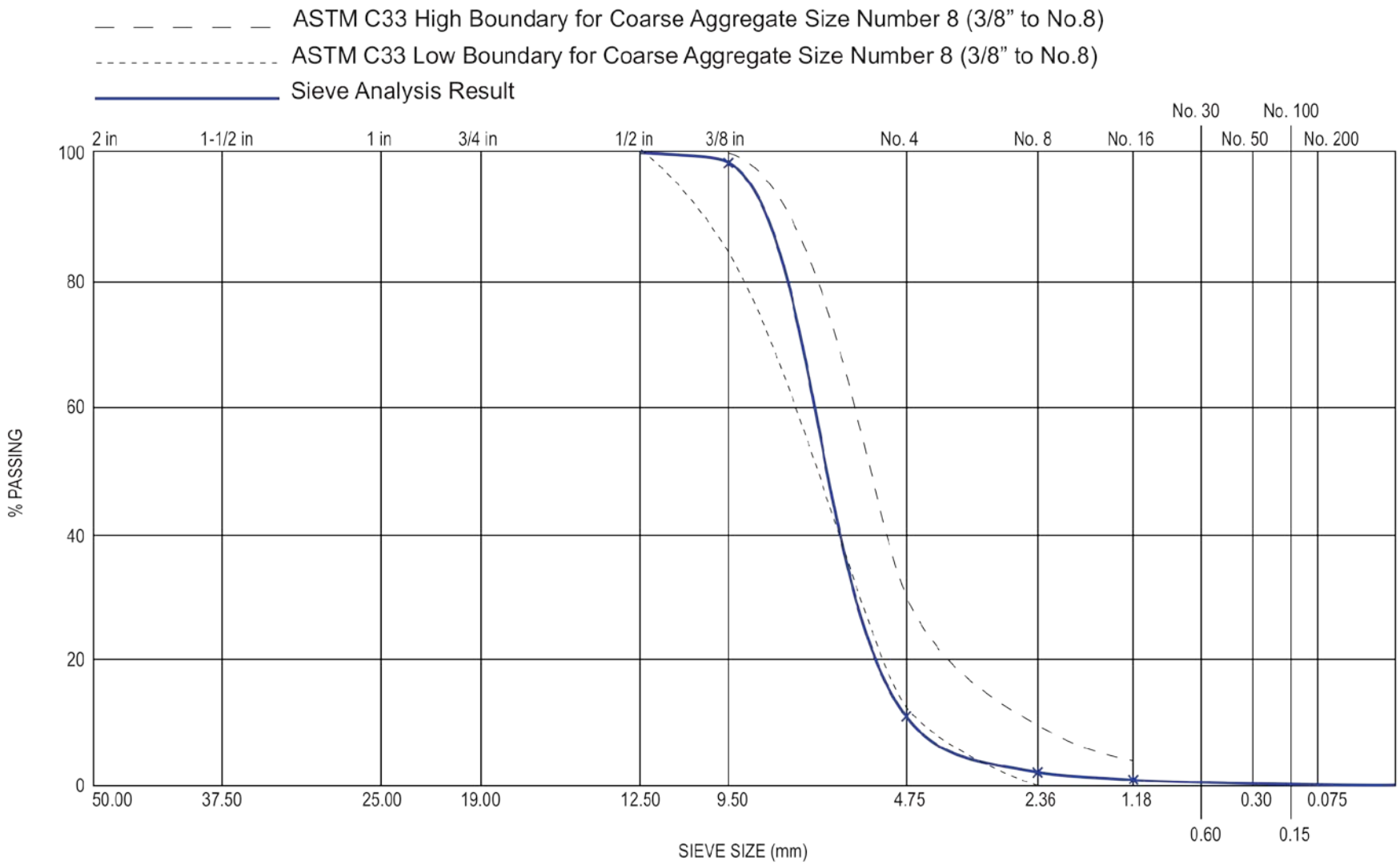

Figure D-3. Aggregate size distribution graph for coarse aggregate no. 8

APPENDIX E
PHOTOGRAPHS OF CRUSHED SAMPLES and COMPRESIVE STRENGTH TEST GRAPHS AS PRODUCED BY THE HYDRAULIC UNIVERSAL TESTING MACHINE

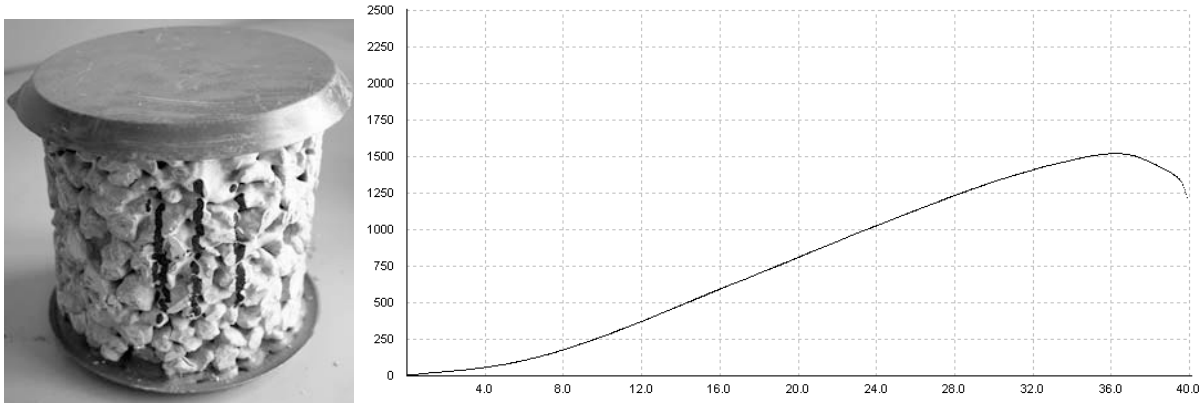

Figure E-1. Sample 111 with graph showing its compressive strength (psi) vs. time (s). The maximum (unadjusted) psi achieved was 1523 at approximately 37 seconds.

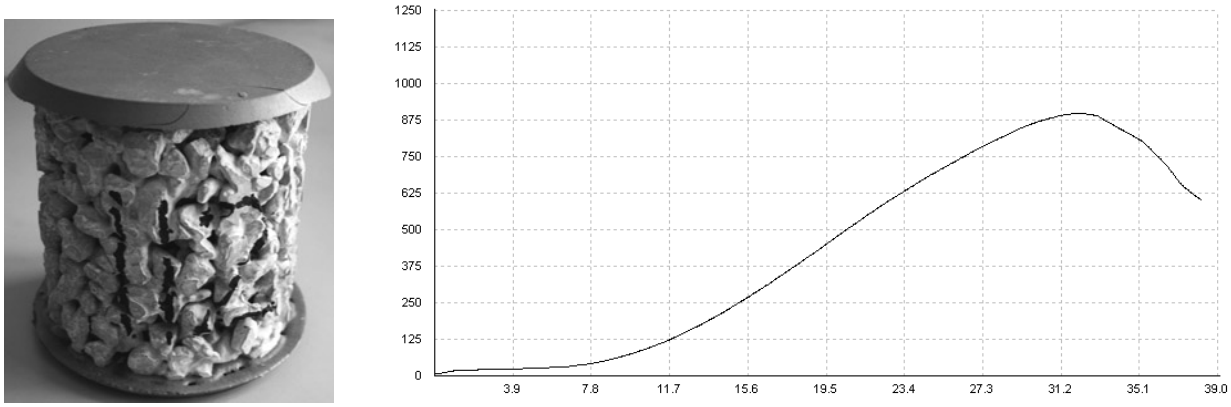

Figure E-2. Sample 112 with graph showing its compressive strength (psi) vs. time (s). The maximum (unadjusted) psi achieved was 897 at approximately 32 seconds.

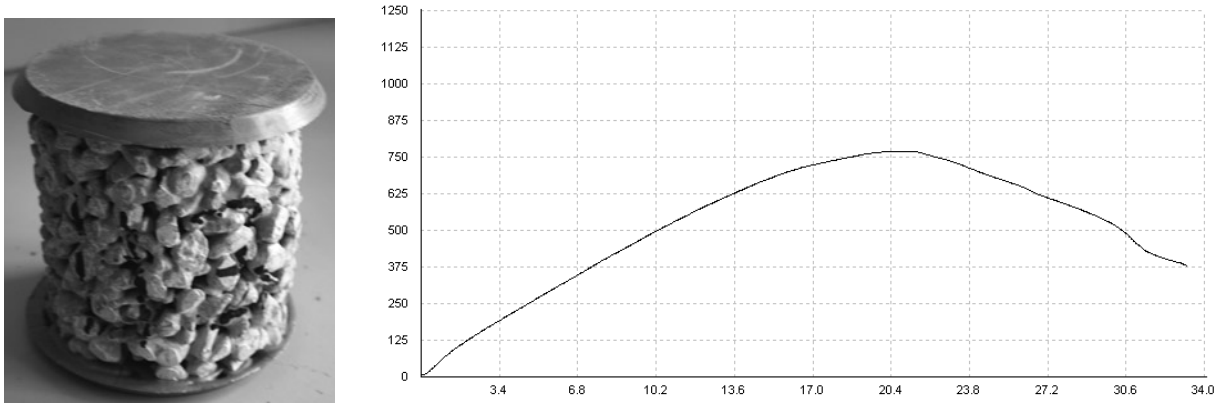

Figure E-3. Sample 113 with graph showing its compressive strength (psi) vs. time (s). The maximum (unadjusted) psi achieved was 769 at approximately 21 seconds.

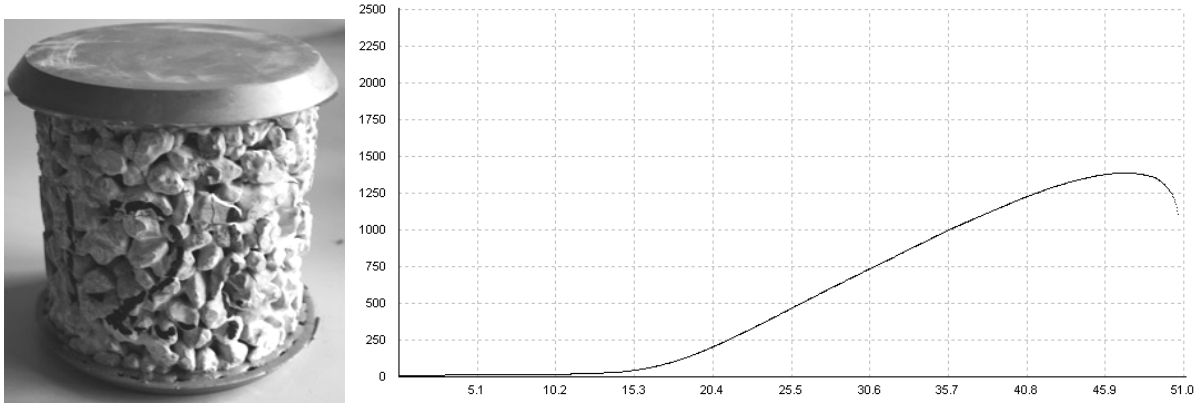

Figure E-4. Sample 121 with graph showing its compressive strength (psi) vs. time (s). The maximum (unadjusted) psi achieved was 1388 at approximately 46 seconds.

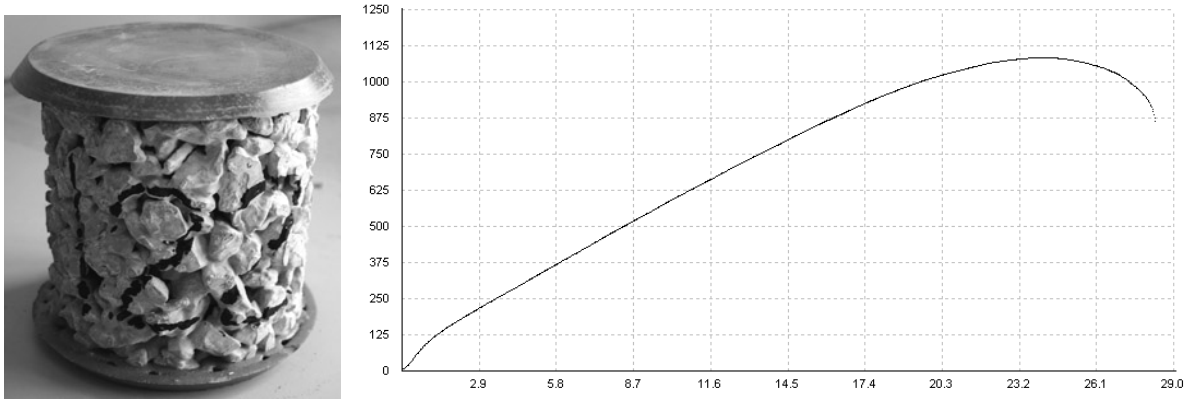

Figure E-5. Sample 122 with graph showing its compressive strength (psi) vs. time (s). The maximum (unadjusted) psi achieved was 1083 at approximately 24 seconds.

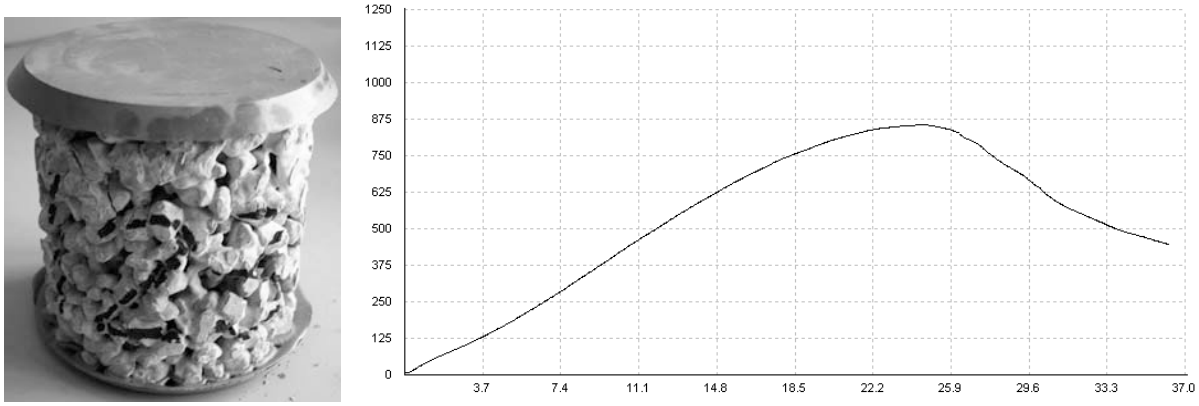

Figure E-6. Sample 123 with graph showing its compressive strength (psi) vs. time (s). The maximum (unadjusted) psi achieved was 855 at approximately 24 seconds.

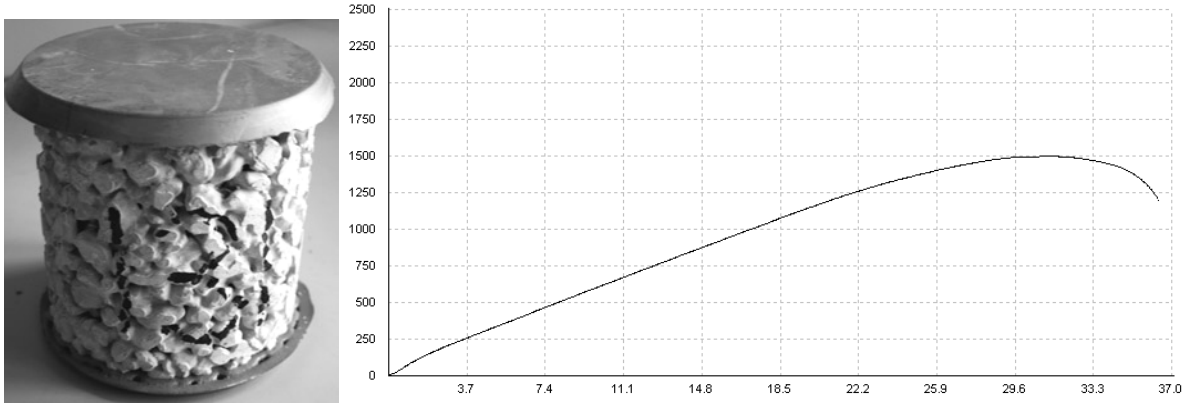

Figure E-7. Sample 131 with graph showing its compressive strength (psi) vs. time (s). The maximum (unadjusted) psi achieved was 1496 at approximately 31 seconds.

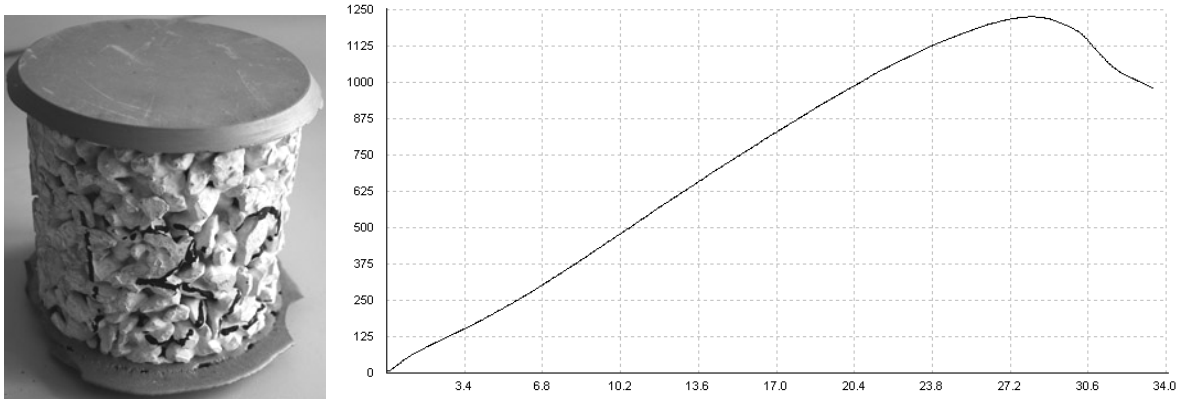

Figure E-8. Sample 132 with graph showing its compressive strength (psi) vs. time (s). The maximum (unadjusted) psi achieved was 1226 at approximately 28 seconds.

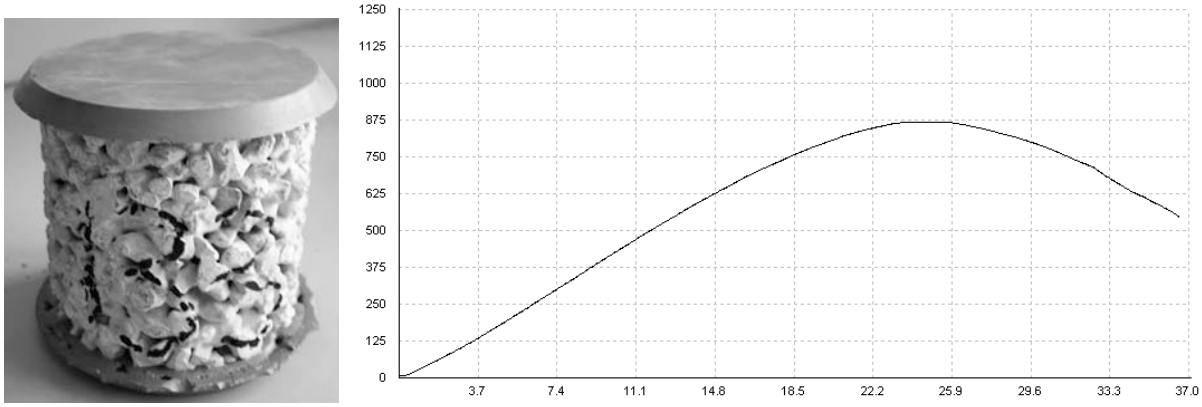

Figure E-9. Sample 133 with graph showing its compressive strength (psi) vs. time (s). The maximum (unadjusted) psi achieved was 868 at approximately 25 seconds.

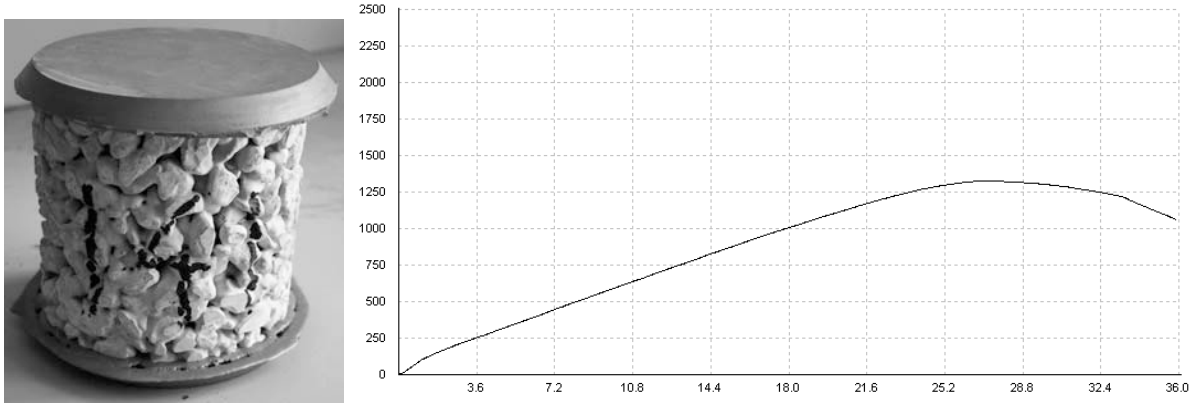

Figure E-10. Sample 141 with graph showing its compressive strength (psi) vs. time (s). The maximum (unadjusted) psi achieved was 1325 at approximately 27 seconds.

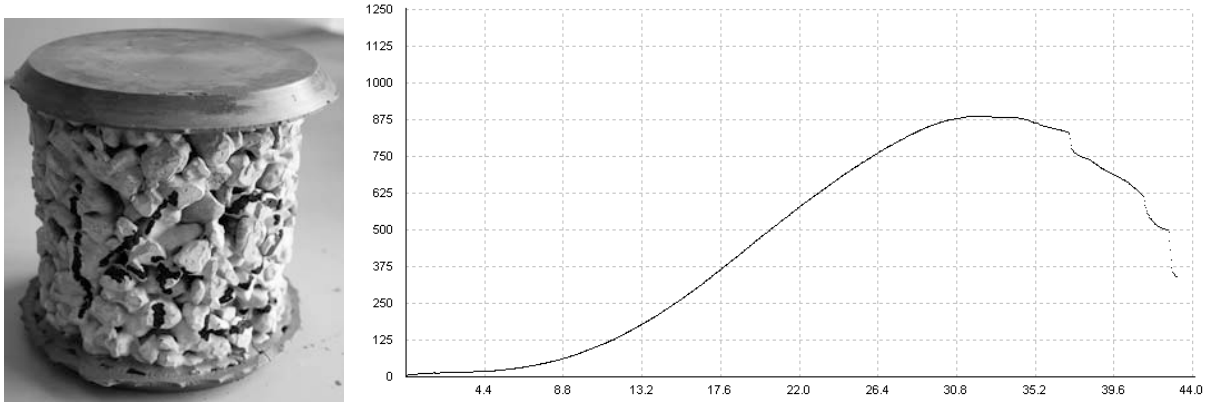

Figure E-11. Sample 142 with graph showing its compressive strength (psi) vs. time (s). The maximum (unadjusted) psi achieved was 886 at approximately 32 seconds.

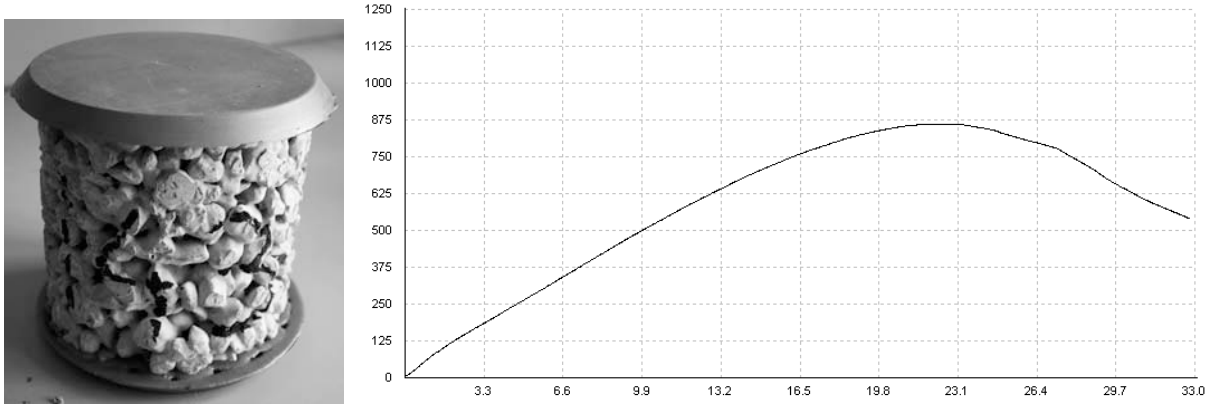

Figure E-12. Sample 143 with graph showing its compressive strength (psi) vs. time (s). The maximum (unadjusted) psi achieved was 860 at approximately 23 seconds.

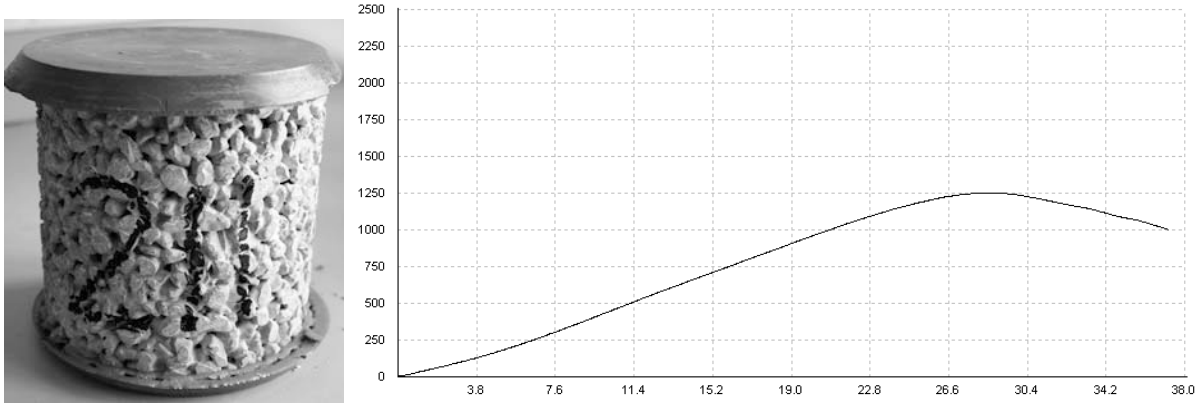

Figure E-13. Sample 211 with graph showing its compressive strength (psi) vs. time (s). The maximum (unadjusted) psi achieved was 1251 at approximately 28 seconds.

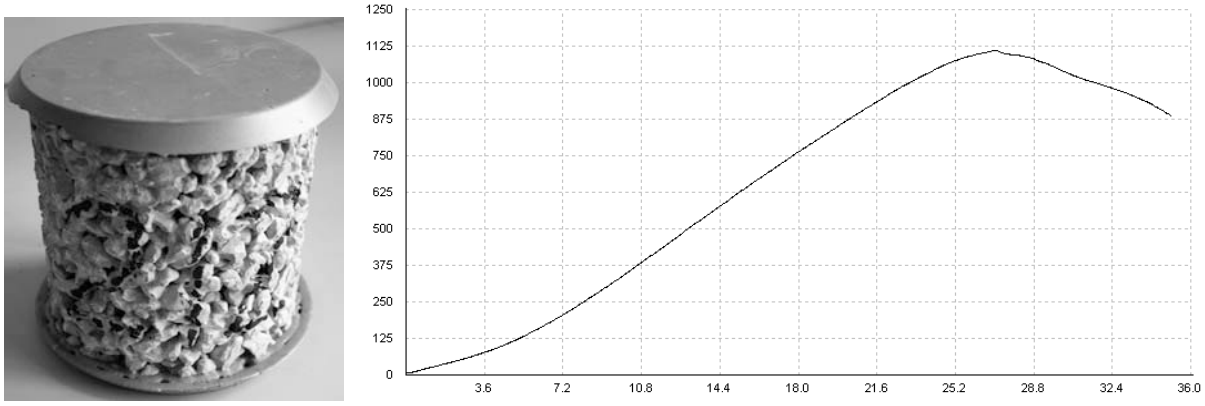

Figure E-14. Sample 212 with graph showing its compressive strength (psi) vs. time (s). The maximum (unadjusted) psi achieved was 1109 at approximately 27 seconds.

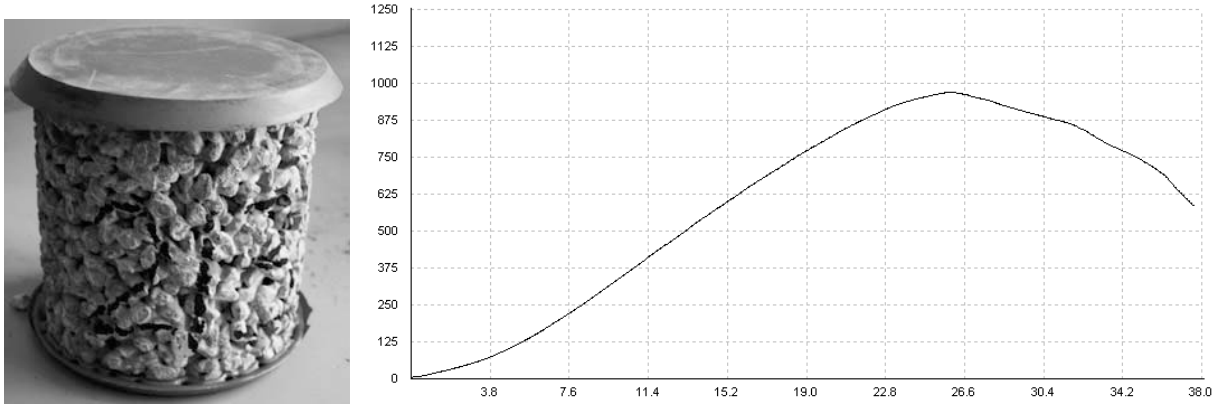

Figure E-15. Sample 213 with graph showing its compressive strength (psi) vs. time (s). The maximum (unadjusted) psi achieved was 968 at approximately 25 seconds.

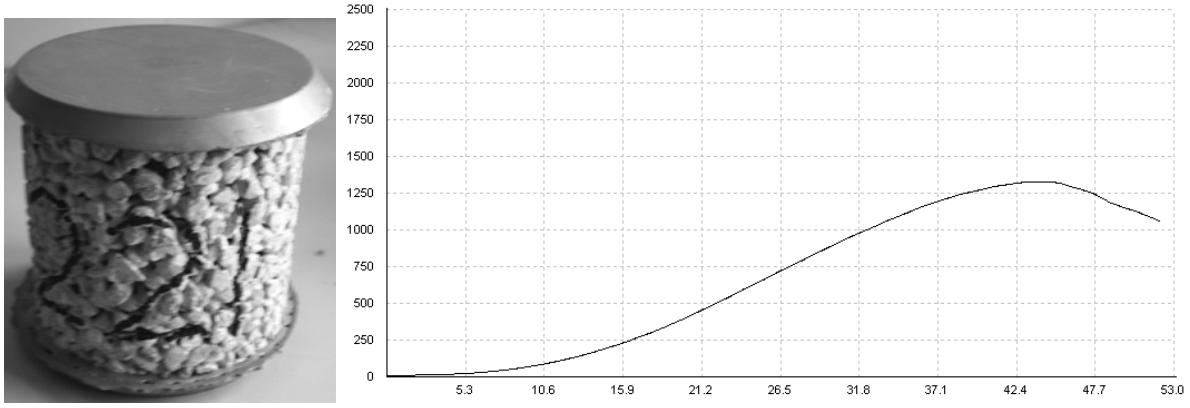

Figure E-16. Sample 221 with graph showing its compressive strength (psi) vs. time (s). The maximum (unadjusted) psi achieved was 1327 at approximately 43 seconds.

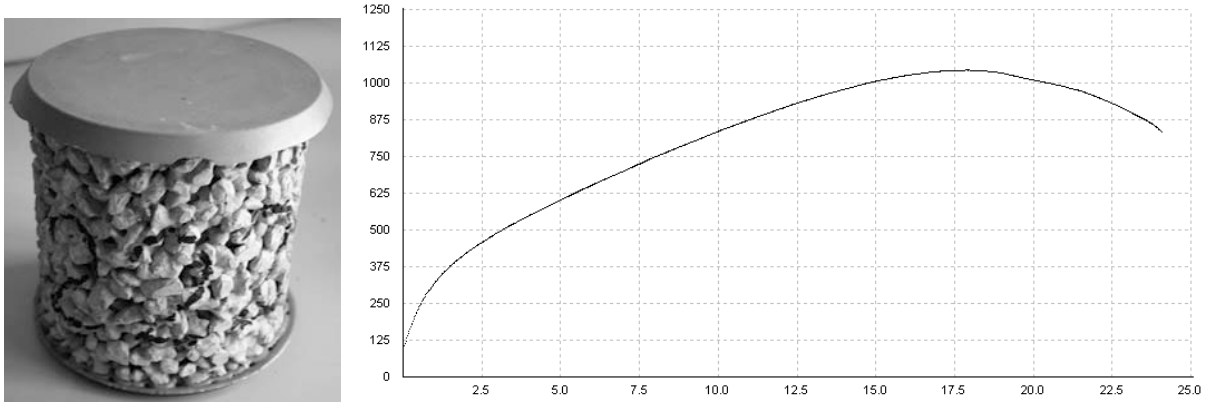

Figure E-17. Sample 222 with graph showing its compressive strength (psi) vs. time (s). The maximum (unadjusted) psi achieved was 1043 at approximately 18 seconds.

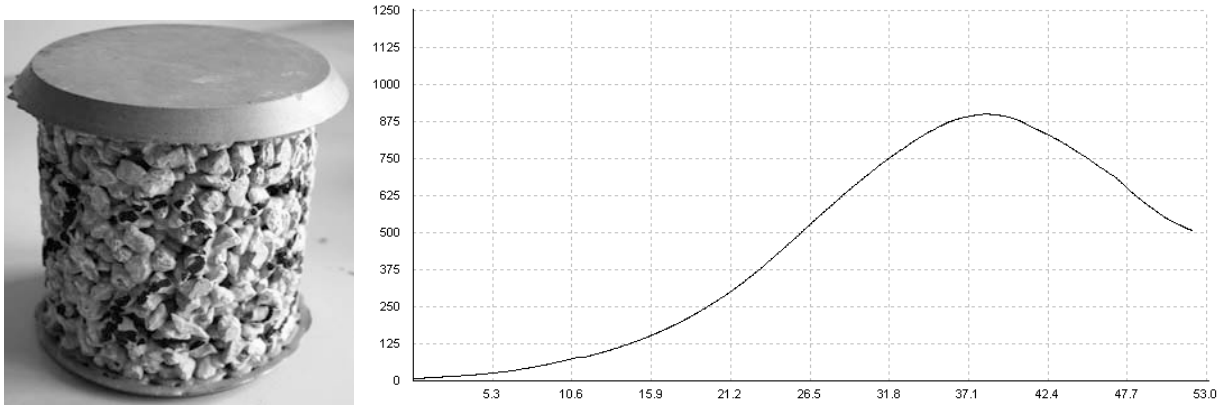

Figure E-18. Sample 223 with graph showing its compressive strength (psi) vs. time (s). The maximum (unadjusted) psi achieved was 900 at approximately 38 seconds.

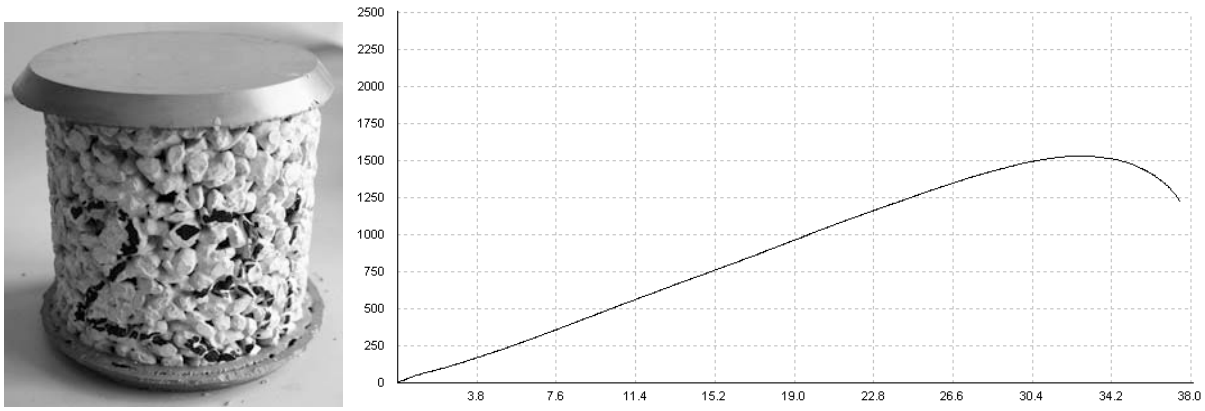

Figure E-19. Sample 231 with graph showing its compressive strength (psi) vs. time (s). The maximum (unadjusted) psi achieved was 1529 at approximately 32 seconds.

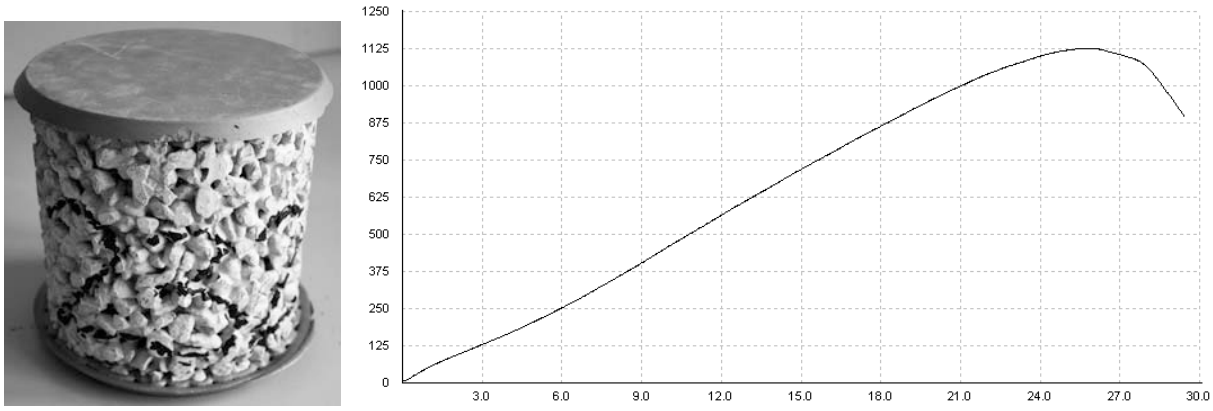

Figure E-20. Sample 232 with graph showing its compressive strength (psi) vs. time (s). The maximum (unadjusted) psi achieved was 1124 at approximately 26 seconds.

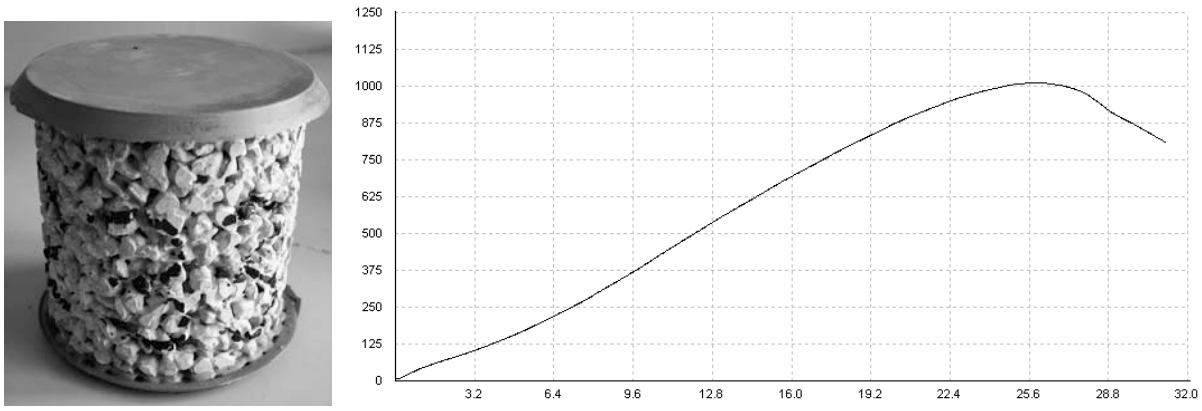

Figure E-21. Sample 233 with graph showing its compressive strength (psi) vs. time (s). The maximum (unadjusted) psi achieved was 1011 at approximately 26 seconds.

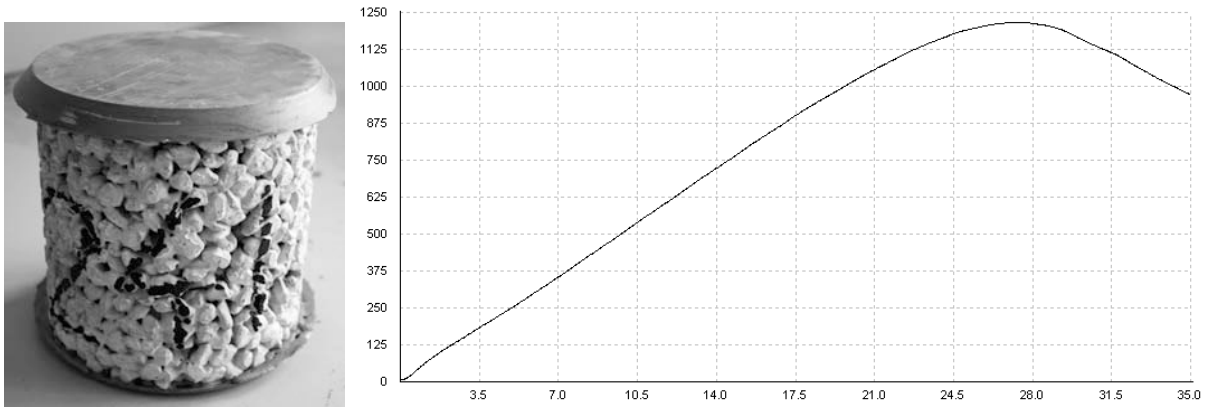

Figure E-22. Sample 241 with graph showing its compressive strength (psi) vs. time (s). The maximum (unadjusted) psi achieved was 1217 at approximately 27 seconds.

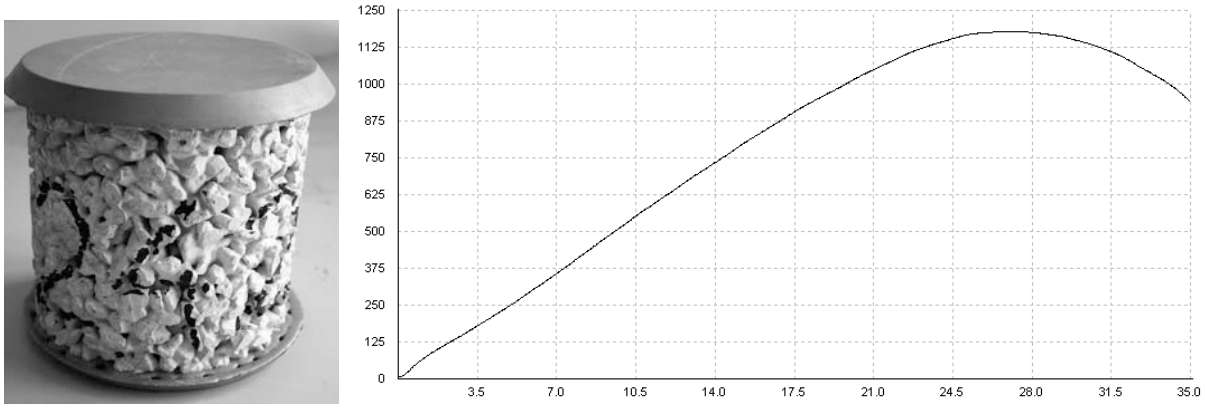

Figure E-23. Sample 242 with graph showing its compressive strength (psi) vs. time (s). The maximum (unadjusted) psi achieved was 1178 at approximately 25 seconds.

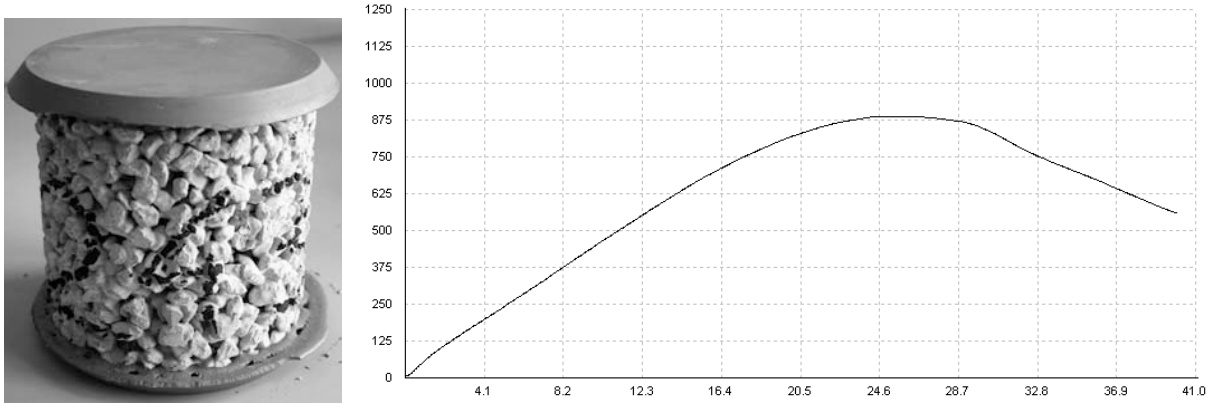

Figure E-24. Sample 243 with graph showing its compressive strength (psi) vs. time (s). The maximum (unadjusted) psi achieved was 886 at approximately 25 seconds.

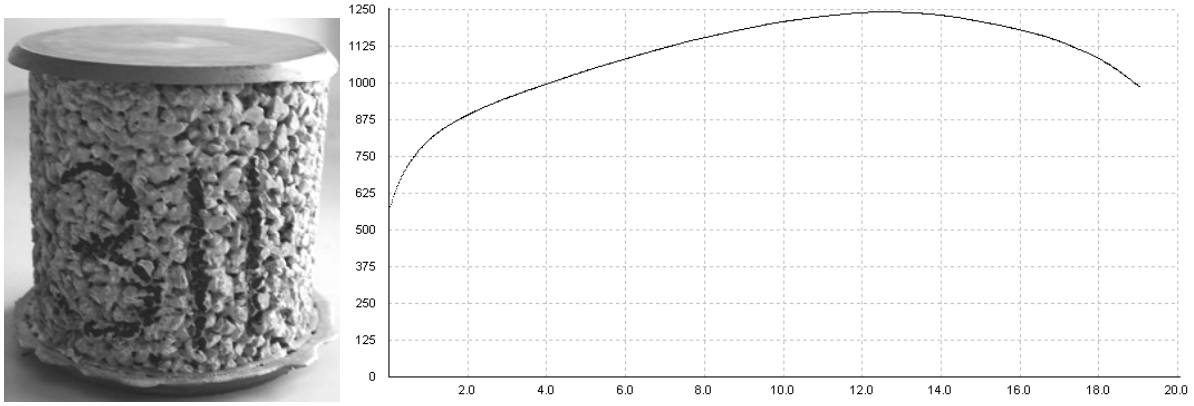

Figure E-25. Sample 311 with graph showing its compressive strength (psi) vs. time (s). The maximum (unadjusted) psi achieved was 1241 at approximately 13 seconds.

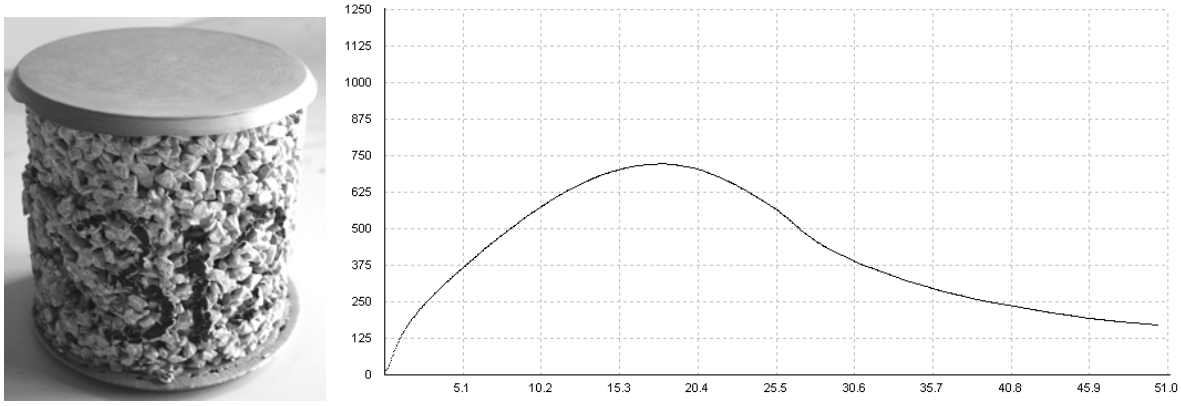

Figure E-26. Sample 312 with graph showing its compressive strength (psi) vs. time (s). The maximum (unadjusted) psi achieved was 721 at approximately 17 seconds.

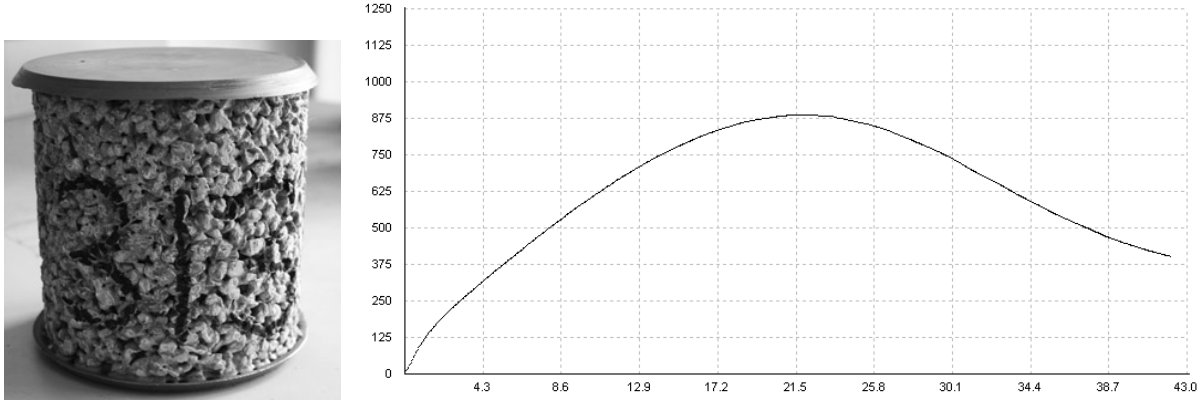

Figure E-27. Sample 313 with graph showing its compressive strength (psi) vs. time (s). The maximum (unadjusted) psi achieved was 885 at approximately 22 seconds.

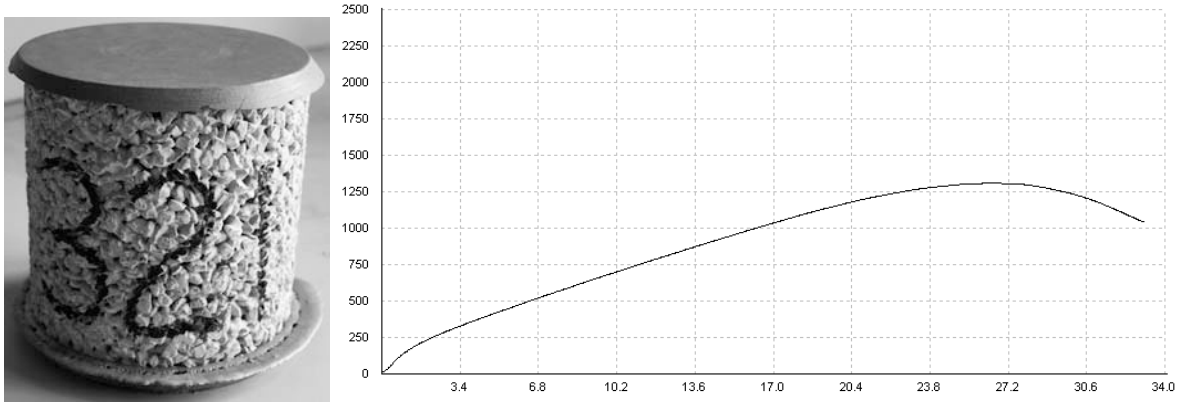

Figure E-28. Sample 321 with graph showing its compressive strength (psi) vs. time (s). The maximum (unadjusted) psi achieved was 1306 at approximately 27 seconds.

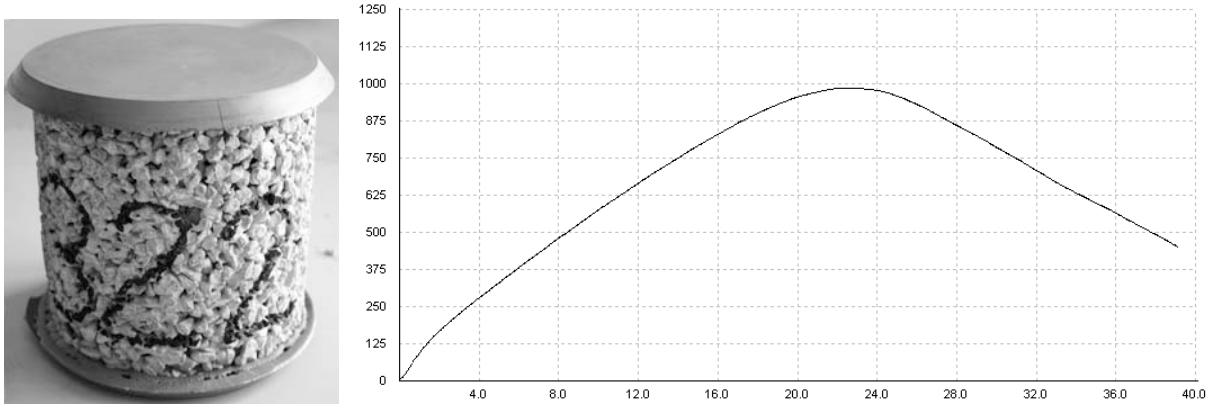

Figure E-29. Sample 322 with graph showing its compressive strength (psi) vs. time (s). The maximum (unadjusted) psi achieved was 985 at approximately 22 seconds.

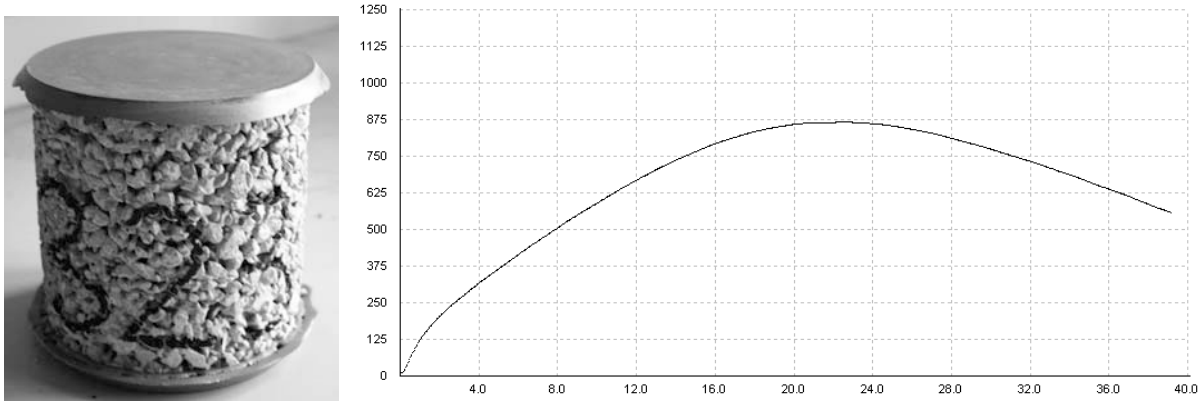

Figure E-30. Sample 323 with graph showing its compressive strength (psi) vs. time (s). The maximum (unadjusted) psi achieved was 866 at approximately 23 seconds.

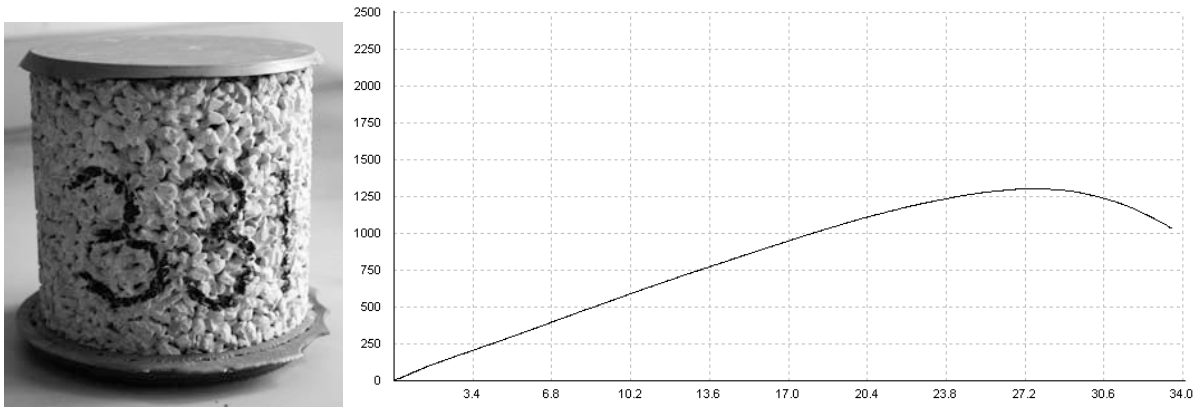

Figure E-31. Sample 331 with graph showing its compressive strength (psi) vs. time (s). The maximum (unadjusted) psi achieved was 1301 at approximately 28 seconds.

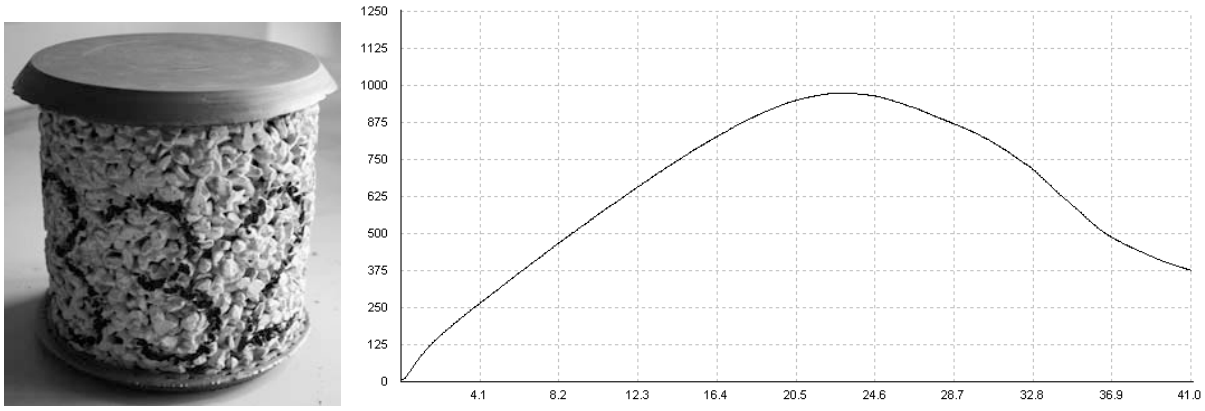

Figure E-32. Sample 332 with graph showing its compressive strength (psi) vs. time (s). The maximum (unadjusted) psi achieved was 973 at approximately 22 seconds.

Figure E-33. Sample 333 was damaged during sulfur capping and was therefore not tested for compressive strength.

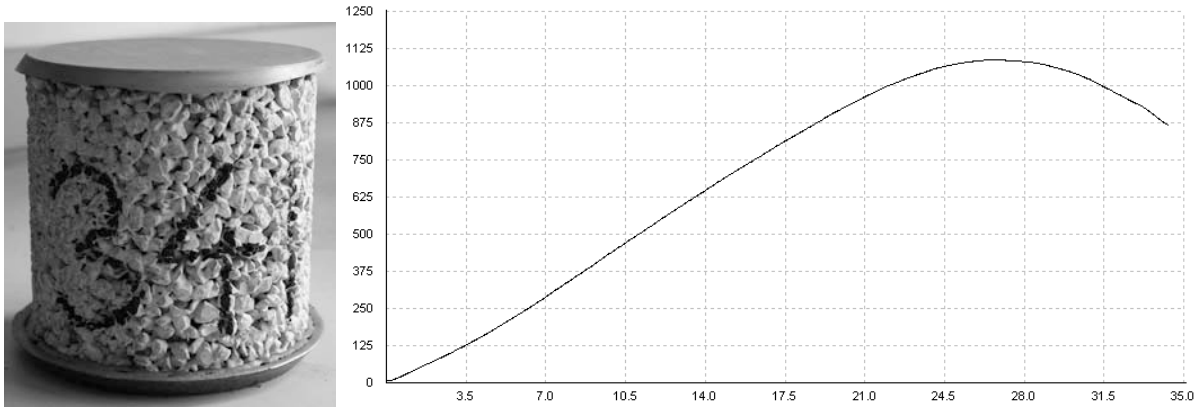

Figure E-34. Sample 341 with graph showing its compressive strength (psi) vs. time (s). The maximum (unadjusted) psi achieved was 1086 at approximately 27 seconds.

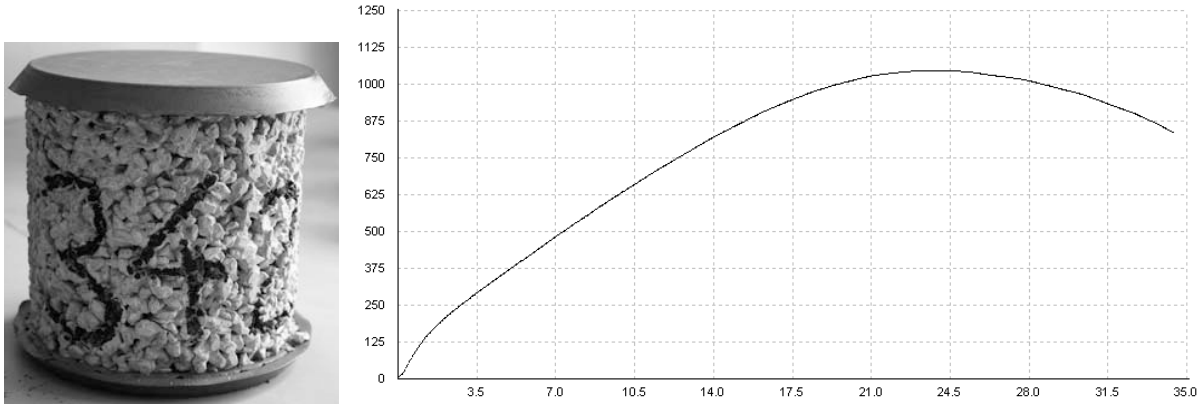

Figure E-35. Sample 342 with graph showing its compressive strength (psi) vs. time (s). The maximum (unadjusted) psi achieved was 1046 at approximately 24 seconds.

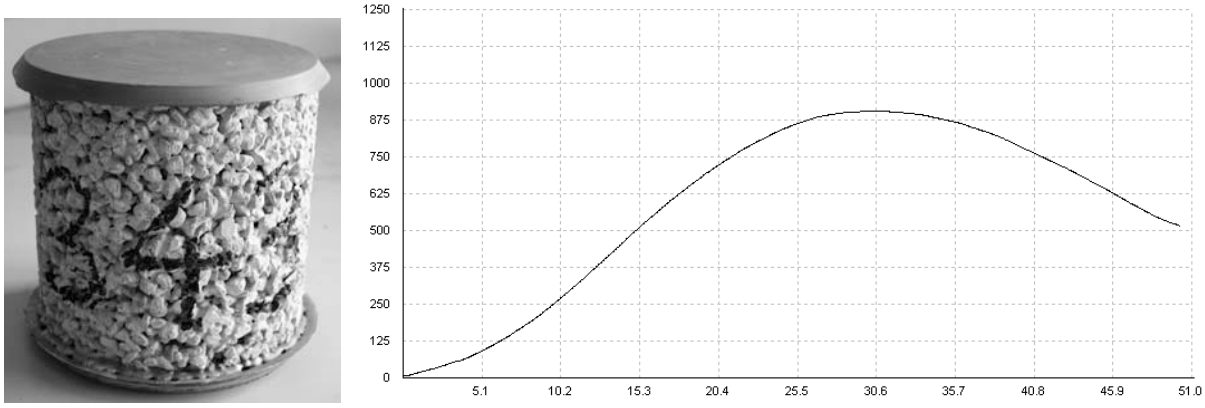

Figure E-36. Sample 343 with graph showing its compressive strength (psi) vs. time (s). The maximum (unadjusted) psi achieved was 903 at approximately 31 seconds.

APPENDIX F
BOTTOM VIEW OF PERVIOUS CONCRETE SAMPLES FROM 111 TO 143

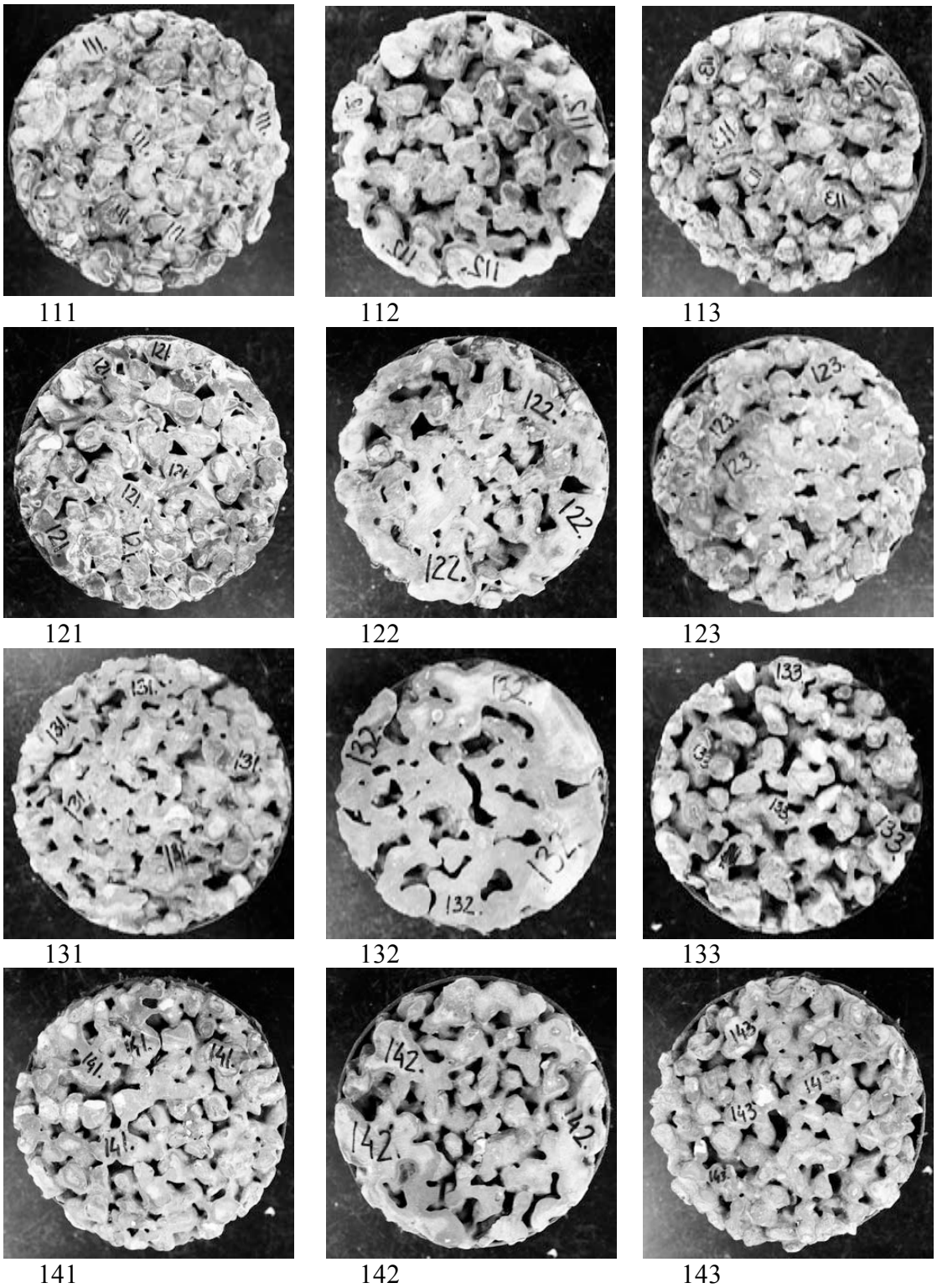

Figure F-1. Bottom view of pervious concrete samples 111 to 143

APPENDIX G
BOTTOM VIEW OF PERVIOUS CONCRETE SAMPLES FROM 211 TO 243

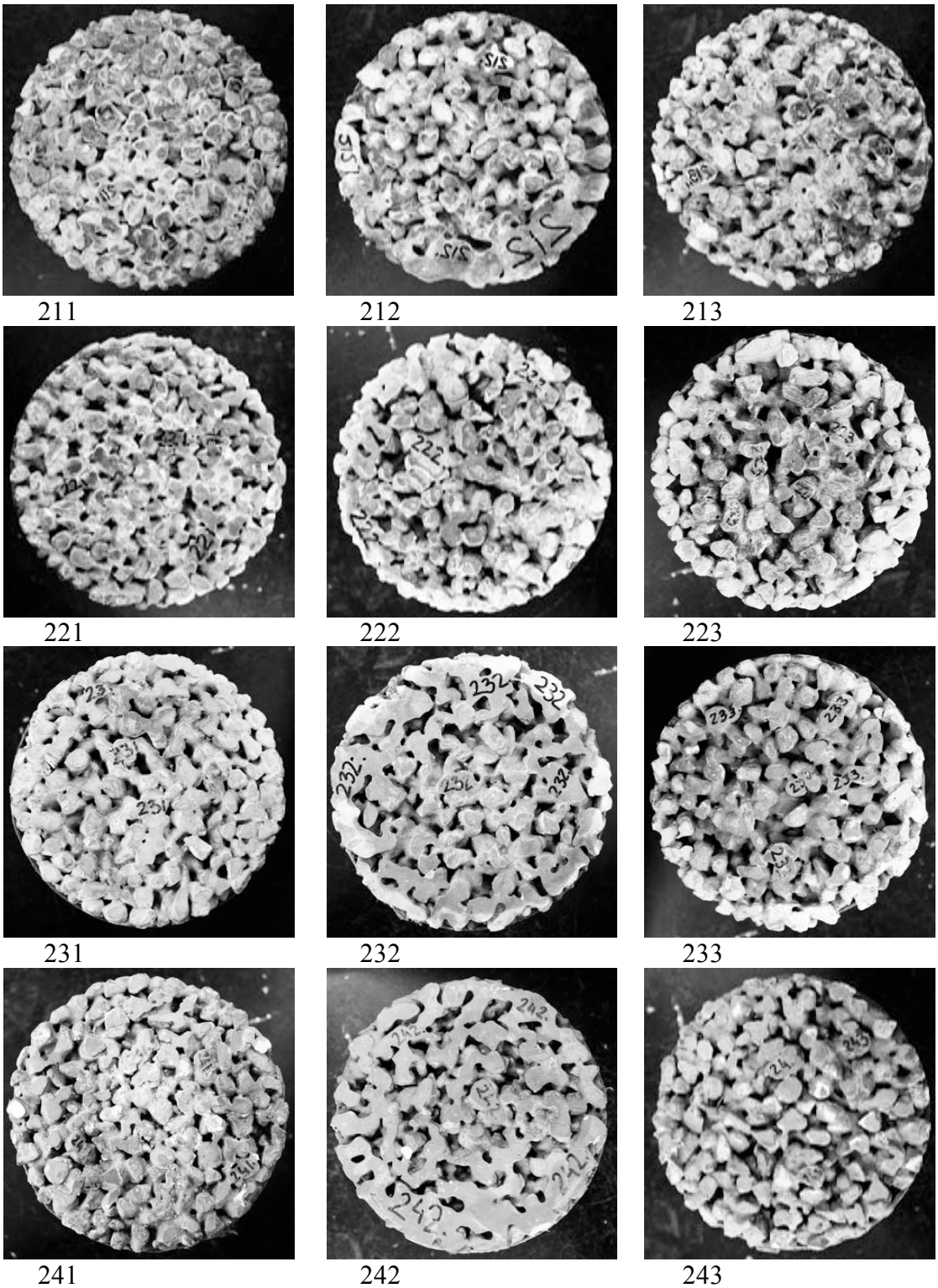

Figure G-1. Bottom view of pervious concrete samples 211 to 243

APPENDIX H
BOTTOM VIEWS OF PERVIOUS CONCRETE SAMPLES FROM 311 TO 343

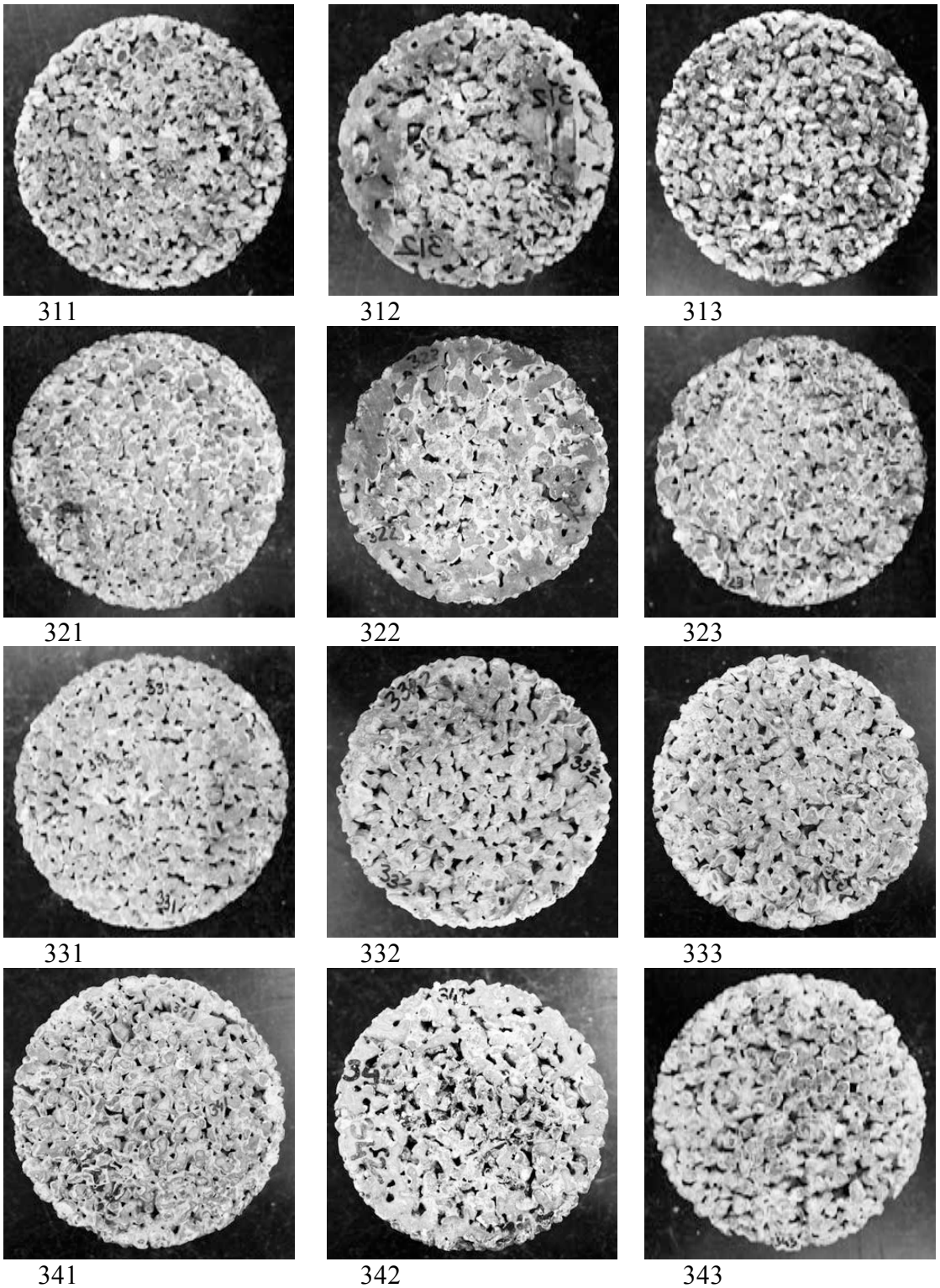

Figure H-1. Bottom view of pervious concrete samples 311 to 343

LIST OF REFERENCES

American Concrete Institute (ACI) (2006). "Pervious Concrete." ACI 522R-06

ASTM Int'l Issues (2009). "ASTM C 1688/C 1688M - Pervious Concrete Test Method." HIS <http://aec.ihs.com/news/astm/2009/astm-pervious-concrete-1909.htm> (May 16, 2009)

Chapman, E. (2002). "Nature's Hideaway: Development & Environment Benefit from Pervious Pavement." <http://www.concreteresources.net/ images/graphics/Hideaway_Development_in_Florida.pdf.> (May 14, 2009)

Chopra, M., Wanielista, M., and Mulligan, A. M. (2007). "Compressive Strength of Pervious Concrete Pavements." Florida Department of Transportation (FDOT), *Final Report FDOT Project BD521-02*: Performance Assessment of Portland Cement Pervious Pavement.

Crouch, L.K., Pitt, J., and Hewitt, R. (2007). "Aggregate Effects on Pervious Portland Cement Concrete Static Modulus of Elasticity." J. Mat. In Civ. Engrg. 19(7), 561-568

Diniz, E.V. (1980). "Porous Pavement." United States Environmental Protection Agency – 600/2-80-135

The Environmental Council of Concrete Organizations (ECCO), 1999. "Information: Recycled Concrete and Masonry".

Ghafoori, N., and Dutta, S. (1995a). "Laboratory Investigation of Compacted No-Fines Concrete for Paving Materials." J. Mat. in Civ. Engrg. 7(3), 183-191

Ghafoori, N., and Dutta, S. (1995b). "Building and Nonpavement Application of No-Fines Concrete." J. Mat. in Civ. Engrg. 7(4), 286-289

Glacier Northwest (2002). "Pervious Concrete Pavements." <https://resources.myeporia.com/company_111/RM%20Topics%20%20Pervious%20Concrete%20Pavements.pdf > (May 19, 2009)

Malhotra, V.M. (1976). "No-Fines Concrete – Its Properties and Applications." ACI J. 73 (11), 628-544

Meininger, R.C. (1988). "No-Fines Pervious Concrete for Paving." Concrete International 10(8), 20-27

Meininger, R.C. (2004). "Pavements that leak." Rock Products <http://rockproducts.com/mag/rock_pavements_leak/> (July 4, 2009)

Mitchell, D.C. (1999). "Advocating Pervious Concrete." Concrete Construction 51(4), 38

Montes, F., Haselbach, L.(2006). "Measuring Hydraulic Conductivity in Pervious Concrte." Enviro. Engrg. Sci. 23 (6), 960-969.

Neithalath, M., Weiss, J., and Olek, J. (2003). "Development of Quiet and Durable Porous Portland Cement Concrete Paving Materials." Final Report, The Institute For Safe, Quiet, and Durable Highways.

Obla, K. H. (2007). "Recent Advances in Concrete Technology: Pervious Concrete for Sustainable Development." <http://www.nrmca.org/research/Pervious%20recent%20advances%20in%20concrete%20technology0707.pdf.> (May 14, 2009)

Palmer, W. D. Jr. (2009). "Testing Pervious Concrete: Fro successful installations, make sure you're getting the right mix." Concrete Construction Online, <http://www.concreteconstruction.net/industrynews.asp?sectionID=985&articleID=936324&artnum=2> (May 13, 2009)

Portland Cement Association (PCA), "Materials: Recycled Aggregates", <http://www.cement.org/tech/cct_aggregates_recycled.asp> (July 2, 2009)

U.S Department of Transportation Federal Highway Administration. "Focus: Recycled Concrete Study Identifies Current Uses, Best Practices" <http://www.tfhrc.gov/focus/apr04/01.htm> (July 4, 2009)

United States Environmental Protection Agency (EPA) (1999). "Porous Pavement." EPA 832-F-99-023: Storm Water Technology Fact Sheet.

Wang, K., Schaefer, V. R., Kevern, J. T., and Suleiman, M. T. (2006). "Development of Mix Proportion for Functional and Durable Pervious Concrete." NRMCA Concrete Technology Forum: Focus on Pervious Concrete, Nashville, TN.

.

BIOGRAPHICAL SKETCH

In 1982, Kristyna Tylova Lannon was born to Zdenka Tylova and Miroslav Tyl, in the city of Brno in the Czech Republic. Kristyna relocated to the United States with her older sister Katerina at the age of 16 years. In 2005 she graduated with honors from the Ringling School of Art and Design in Sarasota, FL with Bachelors in Fine Arts major in Interior Design and minor in Sculpture. A year later, she married a successful skateboarder, Jimmy Lannon. In 2007, Kristyna was accepted to the Masters of Science in Building Construction program, at the M.E. Rinker, Sr. School of Building Construction at the University of Florida in Gainesville, FL. After successfully finishing her Masters degree, she was accepted to the PhD program at the University of Florida.